Tolksdorf, J. F., Kaiser, K., Petr, L., Herbig, C., Kočár, P., Heinrich, S., Wilke, F., Theuerkauf, M., Fülling, A., Schubert, M., Schröder, F., Křivánek, R., Schulz, L., Bonhage, A., Hemker, C. (2020): Past human impact in a mountain forest: geoarchaeology of a medieval glass production and charcoal hearth site in the Erzgebirge, Germany. - Regional Environmental Change, 20, 71.

https://doi.org/10.1007/s10113-020-01638-1

Past human impact in a mountain forest: geoarchaeology of a medieval glass production and charcoal hearth site in the Erzgebirge, Germany

Johann Friedrich Tolksdorf[1], Knut Kaiser[2], Libor Petr[3], Christoph Herbig[4], Petr Kočár[5], Susann Heinrich[6], Franziska D. H. Wilke[2], Martin Theuerkauf[7], Alexander Fülling[8], Matthias Schubert[9], Frank Schröder[9], Roman Křivánek[5], Lars Schulz[10], Alexander Bonhage[11], Christiane Hemker[9]

[1] Bavarian State Office for Monument Protection, Section Schwaben/Mittelfranken, Klosterberg 8, 86672 Thierhaupten, Germany, johann.tolksdorf@blfd.bayern.de

[2] GFZ German Research Centre for Geosciences, Telegrafenberg, 14473 Potsdam, Germany, kaiserk@gfz-potsdam.de and fwilke@gfz-potsdam.de

[3] Masaryk University, Brno, Department of Botany and Zoology, Kotlářská 2, 611 37 Brno, Czech Republic, petr.libor@gmail.com

[4] University of Frankfurt, Institute of Archaeological Sciences, Postfach 11 19 32, 60054 Frankfurt am Main, Germany, herbig.archaeobot@gmx.de

[5] Czech Academy of Sciences, Institute of Archaeology, Letenská 4, 118 01 Praha 1, Czech Republic, kocar@arup.cas.cz and krivanek@arup.cas.cz

[6] Max Planck Institute for Evolutionary Anthropology, Deutscher Platz 6, 04103 Leipzig, Germany, Susann_Heinrich@eva.mpg.de

[7] University of Greifswald, Institute of Botany and Landscape Ecology, Soldmannstraße 15, 17487 Greifswald, Germany, martin.theuerkauf@uni-greifswald.de

[8] University of Freiburg, Sedimentary Geology and Quaternary Research, Albertstraße 23b, 79104 Freiburg, Germany, alexander.fuelling@geologie.uni-freiburg.de

[9] Archaeological Heritage Office of Saxony, Zur Wetterwarte 7, 01109 Dresden, Germany, Matthias.Schubert@lfa.sachsen.de and Frank.Schroeder@lfa.sachsen.de and Christiane.Hemker@lfa.sachsen.de

[10] TU University of Technology Berlin, Institute for Landscape Architecture and Environmental Planning, Straße des 17. Juni 145, 10623 Berlin, Germany, lars@larsschulz.info

[11] Brandenburg University of Technology Cottbus-Senftenberg, Geopedology and Landscape Development, Siemens-Halske-Ring 8, 03046 Cottbus, Germany, alexander.bonhage@b-tu.de

Abstract

Since the twelfth century, forest areas in the upper reaches of the low mountain ranges of central Europe provided an important source of wood and charcoal especially for mining and smelting as well as glass production. In this case study from a site in the upper Erzgebirge region (Ore Mountains), results from archeological, geophysical, pedo-sedimentological, geochemical,

anthracological, and palynological analyses have been closely linked to allow for a diachronic reconstruction of changing land use and varying intensities of human impact with a special focus on the fourteenth to the twentieth century. While human presence during the thirteenth century can only be assumed from archeological material, the establishment of glass kilns together with quartz mining shafts during the fourteenth century has left behind more prominent traces in the landscape. However, although glass production is generally assumed to have caused intensive deforestation, the impact on this site appears rather weak compared to the sixteenth century onwards, when charcoal production, probably associated with emerging mining activities in the region, became important. Local deforestation and soil erosion has been associated mainly with this later phase of charcoal production and may indicate that the human impact of glass production is sometimes overestimated.

Keywords: LiDAR, Forest clearance, glasswork, mining, pollen analysis, soil erosion

Introduction

Mountain areas have been out of the scope of most geoarchaeological studies for several methodical problems: From the archeological point of view, sites are very difficult to identify in these often forested regions with low construction activities and most of the sites identified derive from rather episodic and specialized use (Gassiot Ballbè et al. 2016). Hence, the spatial and chronological resolution of human impact over a longer period of time is difficult to reconstruct. From the aspect of palaeoenvironmental proxies, mountain areas are characterized by local sedimentation systems, often disturbed by catastrophic events, that either need to be studied by combining a number of discontinuous colluvial layers (Larsen et al. 2013) or by using more continuous off-site records like peats or alluvial sediments (Matschullat et al. 1997; Bebermeier et al. 2018). In spite of these methodical obstacles, recent studies have highlighted the importance of peripheral areas, such as mountain ranges, mires, and sandy areas, either to supply medieval to pre-industrial centers with raw materials (ores, timber, tar) and energy (charcoal) (Knapp et al. 2013; Raab et al. 2015; Py-

Saragaglia et al. 2017), or to produce energy-consuming goods like potash and glass (Cílová and
60 Woitsch 2012; Östlund et al. 1998; Kirsche 2014). While previous studies have focused on the technology and composition of different Late Medieval glass types and their attribution to distinct regions in Germany (Wedepohl and Simon 2010) or Bohemia (Cílová and Woitsch 2012; Cílová et al.
63 2015), case studies on the spatial organization of the glass production sites and their environmental impact including geoarchaeological research and geophysical prospection are rather cursory in Bohemia (Křivánek 1995; Schmitt et al. 2006; Seidel et al. 2013; Horák and Klír 2017) but also beyond
66 (Riols 1992). Although these activities must have triggered drastic changes in the local environment, historical sources often underestimate the development in these peripheral areas (Garnier 2000; Durand 2016) and archeological evidence is confined to structures like charcoal hearths or small
69 activity areas, today mostly covered by dense forest (Schmidt et al. 2016). The Erzgebirge region (Ore Mountains) (Fig. 1a) remained largely uninhabited until the onset of rural colonization (Billig and Geupel 1992) began in the mid-twelfth century, and accelerated during the last quarter of the
72 twelfth century due to the discovery of silver ore and the granting of privileges to flourishing mining centers like Freiberg (Richter 2013; Tolksdorf et al. 2018). In the course of this medieval economic development, a considerable number of glass kilns were established in the area with glass production
75 remaining an important business until modern times (Černá 1996, 2014). Situated at the border zone between East-Germany (GDR) and Czechoslovakia, research activities were low for nearly half a century (1945–1990). Only recently has research by the German-Czech EU-project ArchaeoMontan
78 2018 been able to greatly improve our understanding of the emergence of the mining centers and their environmental impact (Tolksdorf et al. 2015, 2018). However, information on the development of more peripheral areas with specialized industries like glass production is still scarce. Using the site
81 of Ullersdorf in the Erzgebirge as a local case study provides the opportunity to develop a diachronic model of the human impact on the surroundings by comparing the changes of vegetation and landscape based on the palynological, anthracological, and sedimentological record with data on
84 historic land use deriving from archeological evidence, remote sensing, and geochemical analyses of

the produced raw materials (glass and charcoal). Comparison on this very local scale may help to quantify human impact during distinct stages of land use and to understand chaînes operatoires within these production activities (Mannoni and Giannichedda 2011). The results can be related at a regional scale to identify economic and political incentives that may have been involved. Not only do these results have implications for refining regional history and archeology, but they may also contribute more generally to planning activities and development with long-term environmental perspectives such as forest conversion and adaptation to climate change (e.g., Milad et al. 2011), sectoral environmental modeling (Reinhardt-Imjela et al. 2018), as well as environmental education and participation (e.g., Slavíková et al. 2017).

Archaeological and environmental setting and regional palynological records

The Ullersdorf site (13° 15′ 40″ E, 50° 36′ 32″ N) is located in the middle Erzgebirge region at 730 m a.s.l., about 12 km southeast of the historic mining town Marienberg (Fig. 1b). It lies within the Ullersdorfer Teichbächel stream valley, a tributary of the Schwarze Pockau river (Suppl. 1A). The geological substrate consists of weathered gneiss, which is covered by periglacial deposits including shallow loess layers as well as fluvial, colluvial and telmatic (peat) sediments. The current land use consists mainly of forest plantations dominated by *Picea abies* (Norway spruce) and supplemented by *Fagus sylvatica* (European beech). The present day mean annual temperature and mean annual precipitation at nearby Kühnhaide weather station at 740 m a.s.l. are 5 °C and 790 mm, respectively. Apart from probably only seasonal mining activities (Tolksdorf et al. 2020), there are no indications for permanent prehistoric settlement of these upper reaches. Although historical records are scarce, the initial rural colonization in this region probably took place during the late $12^{th}/13^{th}$ century and was followed by a phase of abandonment during the fourteenth century as indicated for the Hilmersbach site on the Saxonian side (Geupel 1994) and for the Spindelbach site on the Bohemian side (Horák and Klír 2017; Houfková et al. 2019), located north and south of the mountain crest. Fortifications at the Nonnenfelsen and at the Raubschloss Liebenstein sites (Geupel 1984a, 1995) in the Schwarze Pockau river valley guard an important transition corridor towards Bohemia and infer

that the economic development of this area during the late 12th/13th centuries may have been a purposefully conducted process fostered by local authorities (Fig. 1b). The city of Marienberg was founded in 1521 following the discovery of silver ore in this area in 1519 (Wagenbreth 1990). Based on ceramic surface finds from the thirteenth century and the field name of "Ullersdorf," a characteristic name type for medieval colonization villages using the founders name (here deriving from "Ullrich," a German male name), an abandoned medieval settlement has been suggested in this area (Geupel 1990). Surface finds of glass slags and glass crucibles prove glass production at this site. A geomagnetic survey identified at least three glass kilns (Fig. 2b, Křivánek 1995), features that have been discovered at several locations in the upper reaches of the Erzgebirge (Křivánek 1998). The reinvestigation of the site was initiated by the German-Czech project ArchaeoMontan in 2016–2017. Palynological records of the immediate surroundings (Fig. 1b) have been published from the Mothäuser Heide peat bog, ca. 4 km SW of the study site (Lange et al. 2005), covering the Preboreal to the Subatlantic palynostratigraphical period, from the Schwarze Heide peat bog (Schleich 2006; Seifert-Eulen 2016), comprising pollen spectra from the Boreal to the late Subatlantic, as well as the Lehmhaide peat bog (Schlöffel 2010; Seifert-Eulen 2016), covering the Allerød to Subatlantic period, and the Hühnerheide peat bog (Seifert-Eulen 2016), covering the Atlantic to the Subatlantic period. While a chronological model for the Schwarze Heide sequence has been proposed based on four ^{14}C-ages and ^{210}Pb-ages, independent age control was still missing for the Mothäuser Heide sequence. In this study, we present an age-depth model for this key sequence based on five ^{14}C-ages from a replicate core at the same site.

Method and material

Remote sensing, geophysical survey and profile sampling

To identify anthropogenic microrelief structures a digital elevation model (DEM) based on high-resolution LiDAR data (GeoSN/LfA Sachsen) was created for an area of 42 km^2 around the glass kiln

site. The filtered ground points were gridded using LASTools (Isenburg 2014) with a cell size of 0.4 m based on the average spacing of the ground points. Further data processing was carried out using
138 ArcGIS 10.4.1. After smoothing of the grid by application of a lowpass filter and a five times superelevation, a slope relief visualization with stretched values (standard deviation, n = 2.5) and an inverted greyscale was deemed most suitable for identifying charcoal hearths (Fig. 1c). Shaded relief
141 and local relief index maps (Hesse 2010) were used as independent control. Charcoal hearths appear as circular or near-circular structures with different morphologies on DEM-derived maps (Hesse 2010; Deforce et al. 2013). In mountainous regions they are predominantly build into slopes (Nelle
144 2003; Hildebrandt et al. 2007) where they are visible as circular or oval, planar platforms (Suppl. 1B; Raab et al. 2017). Furthermore, we derived an aggregated DEM with a cell size of 20 m to analyze the sites in terms of slope and aspect. The site density was calculated by means of a circular
147 neighborhood (radius = 250 m) around each site and given as sites per km^2. Geophysical measurements on the plateau south of the stream and beside the sunken road tracks (Fig. 2a) had already been conducted in 1993 (Křivánek 1995) using a FM-36 Magnetic Gradiometer (Geoscan
150 research) and are reprocessed for this study. While an area of 40 m × 40 m was measured with a grid-width of 1 m, detailed measurements with a grid width of 0.5 m have been performed on a subarea of 20 m × 17 m where magnetic anomalies appeared most prominent (Fig. 2b). All samples
153 derive from four key profiles (Fig. 2a) that cover different local sedimentary environments. Profile 2 (a replicate of test profile 1 that was not sampled) is situated within a small drained peat area on a stream terrace that was fed by water from a spring horizon at about 90 m distance from the position
156 of the glass kilns. The maximum peat thickness is 80 cm (Suppl. 1C). It was sampled for palynological, pedo-sedimentological, and geochemical analyses by increments of 1 cm in the upper part and 2 cm and 3 cm spacing in the lower part. A thin section for micromorphological analysis was prepared
159 from the transition of the peat layer to the overlying colluvial sediment. Charred material was extracted for ^{14}C-analyses at depths of 14, 16, and 32 cm. Profile 3 is located beside the Ullersdorfer Teichbächel at the opposite site of the glass production area where alluvial and colluvial layers are

intercalated. The profile was sampled for palynological and pedo-sedimentological analyses as well as optically stimulated luminescence (OSL) and micromorphological assessment. Profile 4 was used to resolve the age and to unravel the possible relation of an isolated fall shaft to the glass production. It is situated at the side of the circular mining heap 100 m to the southwest of the glass production site. Profile 5 covers colluvial layers on the downhill slope between the glass kilns and the stream. Archeological material within the profile trench was recovered by stratigraphical units and every unit was sampled for pedo-sedimentological analysis. Ten charcoal hearth plateaus in the immediate vicinity of the site were sampled for anthracological spectra to provide complementary spatial and chronological information about the possible exploitation strategies and deliberate selection of wood species.

Palynological, anthracological and macrobotanical analyses

Samples of 0.5 cm^3 sediment were prepared according to standard acetolyse method (Moore et al. 1991; Berglund and Ralska-Jasiewiczowa 1986). A minimum of 500 palynomorphs was counted for each sample with identification based on the standard literature (Beug 2004). *Lycopodium* spores were added to calculate the pollen concentration (Stockmarr 1971). Local wetland taxa like *Cyperaceae, Alnus, Sphagnum, Caltha*, and *Equisetum* were excluded from the calculation of the pollen sum. Combination of PCA and constraint single link cluster analysis as implemented in PolPal (Nalepka and Walanus 2003) was used for a zonation of the pollen record in profile 2. The number of charcoal particles was recorded without further subdivision into size classes (Clark 1984). To translate the pollen percentages of selected main taxa into an estimation of the vegetation composition, a REVEALS model was calculated using the Rpackage DISQOVER (parameters = peatland, 30 m diameter; see Theuerkauf et al. 2016). Material for anthracological analysis of the charcoal kilns was extracted by dry-sieving of material from different random sampling spots within the features. In general, the kiln features did not allow for the recognition of distinct stratigraphical subdivisions that might reflect several use-phases. A sample of 30 charred pieces was determined to estimate the general composition of the charcoal spectrum. Additionally, subfossil wood embedded

in the fluvial layers and three pieces of charcoal from a colluvial layers in profile 3 were determined based on wood-anatomical features (Schweingruber 1990). Flotation and wet sieving (2, 1, 0.5, 0.25 mm mesh width) was used to retrieve plant macroremains and 14C dating material from peat layers in profile 2 (slices of 1 cm thickness, ca. 100 g peat) at a depth of 10, 14, 16, and 18 cm and from charcoal kiln 1 (3 l). The material was identified according to standard literature (Cappers et al. 2012) and a reference collection of domestic and wild plants.

Radiocarbon analyses, dendrochronology and OSL dating

Radiocarbon (^{14}C) analyses were performed on seven samples by the Curt-Engelhorn-Zentrum für Archäometrie at Mannheim (CEZ) and calibrated according to the IntCal13 dataset (Reimer et al. 2013) (Table 1). The age-depth model for profile 2 was built on the statistical procedure of Haslett and Parnell (2008) implemented in the R-package Bchron (Parnell 2016). Fragments with the maximum amount of visible tree rings were submitted for dendrochronological analyses but provided no results due to irregular growth patterns. A sample for OSL analyses (HUB0749) was extracted from profile 3 using an opaque box. The grain size fraction 90–200 µm was subsequently processed at the Luminescence laboratory of the HU Berlin according to standard procedure. Equivalent dose was measured using a Risø TL/OSL DA-15C/D reader running a SAR protocol (Murray and Wintle 2000) with a preheat of 200 °C. The equivalent dose aliquots showed a distinct skewed distribution that is typical for incomplete bleached sediments. Consequently, a minimum age model (Galbraith et al. 1999) was used for the calculation of the sedimentation age. The dose rate was calculated based on the content of ^{238}U, ^{232}Th, and ^{40}K measured by gamma ray spectroscopy as well as the cosmic dose at the sampling position and depth using the software DRAC (Durcan et al. 2015).

Pedo-sedimentological, micromorphological and geochemical analyses

Soil horizons were recorded and sampled according to the guidelines of the German soil classification standard (AG Boden 2005). A total of 12 samples were subjected to pedosedimentological analyses on the matrix matter < 2 mm (Supplement 4). Grain size distribution was determined after removal

of organic matter by laser diffraction (BeckmanCoulter particle analyzer). Organic matter was estimated by combustion at 550 °C (loss-on-ignition; Heiri et al. 2001). Two thin sections for micromorphological analyses were prepared from the upper layers in profile 2 and profile 3 in order to study the sedimentation milieu and post-depositional alterations. Sediment monoliths were recovered by boxes and impregnated with resin. Microscopic description of features under plain and crossed polarized light refers to the nomenclature of Stoops (2003). Portable X-ray fluorescence (pXRF) measurements were applied on homogenized dried material from the pollen monoliths for a first assessment of vertical element distribution using an Innov X Delta device equipped with a 4 W Rh tube and 25 mm silicon drift detector (SSD) in soil analysis mode (each measurement consists of two 30 s beams). As these measurements are strongly influenced by changes in the soil texture and organic matter as well as their compensation by the measurement mode of the device used, the contents of Zn, Pb, Fe, K, Mn, Cr, and Cu were additionally measured for 14 sample points after complete drying (106 °C), homogenization in a mortar and microwave digestion (ultraCLAVE IV MLS GmbH, with HNO_3 at 240 °C, 100 bar) by inductively coupled plasma–optical emission spectrometry (ICP-OES) using a Spectro Ametec Arcos II device (Side-On Plasma, 1400 W). The results of ICP-OES are given as mean values from triple measurement of the same sample. Although a broad set of elements is available in the profile (Supplement 5), we decided to focus on As and especially Pb as elements that have been established as reliable indicators of regional mining activities (Bohdálková et al. 2018). A specific geochemical signal from potash production cannot be expected as the main component KOH is easily soluble therefore not accumulated in the sediment. We also neglected S as it has been massively introduced into the soils of the region by intensified lignite firing in Bohemia since the 1940s that caused severe forest dieback (Armbruster et al. 2003). Quartz raw material and glass slags have been analyzed by wavelength-dispersive spectrometry (WDS) using a JXA 8230 and JXA 8500F electron microprobe with 15 kV, 20 nA and a 20 µm probe size. Energy-dispersive spectrometry (EDS) was used for pre-characterization to verify that all noticeable elements got measured. For quartz, the SiO_2 content was set to 99.5 wt% and all other elements were measured

quantitatively by WDS. The glass slags have been measured entirely by WDS. Natural minerals such as orthoclase (Si, Al, K), hematite (Fe), albite (Na), diopside (Ca, Mg), rutile (Ti), rhodonite (Mn), apatite (P), naumannite (Ag), chalcopyrite (S), tugtupite (Cl), Cr_2O_3 (Cr), and galena (Pb) were used for calibration. Si and Na were measured simultaneously. Acquisition times on peaks were 10–20 s except for S, P (40 s), Ag (50 s), and Pb (60 s) whereas the background level on both sides of the peak were measured in half of the peak acquisition time. A well-characterized natural volcanic glass from Lipari Island (Italy) was used as cross-reference material.

3D Visualization

To support the overall outcome, a 3D visualization (Lungershausen et al. 2013) was created for five selected time spans (Schulz 2019). Using the software Cinema 4D R19, the DEM data were combined with information about the prevailing vegetation composition and examples for infrastructure associated with land-use activities.

Results

Remote sensing and geophysical survey

In total 348 potential charcoal hearth sites have been identified, of which 6 sites could not be classified within reasonable certainty and were therefore excluded from further analysis. Three groups have been identified: (1) west of the Schwarze Pockau in the Mothäuser Heide with a density of up to 61 sites per km^2, (2) in the direct vicinity of the Ullersdorf glass kiln with a density of up to 81 sites per km^2, and (3) north east of the glass kiln site in the Schwarze Heide with a density of up to 40 sites per km^2 (Fig. 1c). Similar site densities are reported for other low mountain ranges in Germany, e.g., 5–166 sites per km^2 in the Harz (von Kortzfleisch 2009), 40–150 sites per km^2 in the Black Forest (Ludemann 2003, 2011), and 23 sites per km^2 in the Kellerwald (Schmidt et al. 2016). Two morphological types can be recognized: Type 1 are distinctly circular features with a ridge

surrounding the hearth bearing platform (Fig. 1c, inset 1), which are located predominantly in the western aggregation, although individual sites are scattered across the whole area (n=58). A comparable morphology has been described for areas in Belgium (Hardy and Dufey 2015), the Pfälzerwald (Hildebrandt et al. 2007), the Ostharz (Swieder 2019), and Brandenburg (Raab et al. 2019). Type 2 are sites with a typical configuration for slopes (Fig. 1c, inset 2) that can be found evenly distributed in the study area (n=280). Four sites could not be classified morphologically due to disturbances of the relief. Sites with a surrounding ridge are located in areas with lower inclination (mean 3.3° ± 1.5°, range from 0.4° to 8.6°), while the other type of charcoal hearth is generally found on steeper slopes (mean 5.9° ± 1.5°, range from 5.9° to 17°). Most sites with a surrounding ridge are located on steeper slopes with a north-east to south-east aspect, while the charcoal hearths on slopes are predominantly located on north and south facing slopes. The geomagnetic measurement reveals three anomalies in the form of extremely high magnetic values surrounded by strong negative signal values (Fig. 2b, features 1–3). A number of smaller anomalies is present but does not form any clear spatial structure. These anomalies probably derive from slags that scatter near the topsoil. Based on the comparison with geomagnetic features from excavated glass kiln sites in the Erzgebirge, these features 1–3 correspond to typical kiln features in size, shape and signal amplitude (Křivánek 1998, 2001).

Profile 2

Weathered gneiss covered by gneiss blocks in a silty matrix (VI Gr) make up the base of the stratigraphic sequence in profile 2 (Fig. 3). It is overlain by a periglacial solifluction layer (V Gr-Cx horizon). On top, a fine-layered organic gyttja (IV fF) is covered by peat (III fHr). The latter contains well identifiable plant remains, such as sedge roots, mosses and wood. The diminishing mineral fraction is dominated by sand. The wide variation of the calculated total pollen concentration, e.g., at 29 cm depth, indicates that the development of this sediment layer has probably been affected by changing peat growth rates, caused by local desiccation and rewetting. At a depth of 14 cm below the surface, a sharp but undulating transition of a silt-dominated yellow-brown layer with lower

organic content occurs (II Gr-fM). Based on the micromorphological assessment of the thin section, microcharcoals are incorporated both in the peat (Fig. 4A and B) and the overlying layer. Although some signs of in situ bioturbation can be identified in the silt layer, most of the organic material is consisting of partly decomposed and fragmented plant material with visible cell structures, transported together with rounded micro-aggregates from 20 to 100 µm size and no layering can be observed (Fig. 4C). Beside fecal pellets and paraphyses of fungi, an aggregate of *Meliola ellisii* spores, which is a parasite on *Calluna vulgaris* (van Geel et al. 2006; Chambers et al. 2011), was identified (Fig. 4D). The silt-dominated unit II Gr-fM cannot have developed from the peat layer but is allochthonous material that could derive from the nearby slope. Although the micromorphological features do not provide unequivocal evidence for colluvial dynamics, the observed rounded micro-aggregates could support the idea that the material was relocated. The in situ bioturbation does not contradict this idea and could have developed after the deposition of the layer. The uppermost part of the sequence from 9 cm depth is a peat layer (Hv), with a strong silt component. Due to modern drainage, the upper peat layer shows strong signs of mineralization. While wet sieving of the layer at 10 cm depth only retrieved three very small charcoal particles (indet.), sample slices at 14, 16, and 18 cm depth provided very small quantities of charred *Picea abies* needles that were used for ^{14}C-analysis.

The pXRF results show strong increases of Pb and As from the sample depth of 23 to 20 cm and the trend of increasing Pb-contents, peaking between 23 and 14 cm depth, is corroborated by the ICP-OES.

From 78 to 70 cm below the surface, the record is dominated by pollen of shrubs and herbs (Fig. 5). Tree pollen, mostly of pine and birch, make up less than 50% of the terrestrial pollen sum. Pollen attributable to *Corylus* are present in small numbers only. Overall, the pollen record suggests that this section has been deposited during the early Holocene before the main expansion of hazel at 10,600 cal BP (Giesecke et al. 2011). The samples between 63 and 71 cm, however, show less herb pollen and more tree pollen, including pollen of tree taxa related to warmer climate such as *Alnus*,

315 *Tilia*, and *Fagus*. These trees expanded in central Europe only after ca. 10,000 cal BP, i.e., the pollen suggest that this section is younger than the sediments above. However, the processes that could have caused this biostratigraphical inconclusive result in this part of the stratigraphy are not capable. 318 The pollen of tree taxa indicative of a warmer climate might originate from eroded peat layers of earlier interglacials. Alternatively, the age reversals may represent redeposition of sediment layers, perhaps including bioturbation. At ca. 50 cm, increasing percentages of pollen from *Corylus,* followed 321 by the appearance of pollen from trees dependant on warmer climates probably represent the expansion of these tree taxa between 10,600 and 9000 cal BP (Giesecke et al. 2011). The next prominent biostratigraphical features are the sharp increase in pollen from *Picea* at 42 cm and the 324 increase in pollen percentages of *Fagus* and *Abies* at 38 cm. These events are dated at 7300 cal BP and 6000 cal BP, respectively, in the Mothäuser Heide record (Suppl. 4). At this point, very low abundances of shrub and herb pollen show that the area was covered by dense forest vegetation 327 with no recognizable open areas or clearances. A first very weak increase in herb pollen (Poaceae, *Artemisia*, *Asteraseae*) is observed between 32 cm and 26 cm depth (approx. 250–850 cal AD). This can be correlated to the Mothäuser Heide record, which shows elevated pollen percentages of 330 severals herbs, including *Secale*, during this time period. High pollen percentages of e.g. Poaceae and the presence of *Rumex acetosella*-type and *Secale* pollen above 18 cm depth indicates human activity close to the study site at about 1450 cal AD.

333

Profile 3

Profile 3 is located at the transition from the hillslope to the floodplain of the stream valley (Fig. 6; 336 Suppl. 1D). The base of the stratigraphy consists of fluvial sands (VI Cv) covered by dark-gray sand and silts with an upwardly increasing darkhumic layering in the upper part (V M2/3), which contained a crushed piece of quartz. From the northwestern part of the profile a layer of medium to fine- 339 grained sands with charcoal particles (IV M1) is situated on top of this silt layer. Micromorphological

analysis (Fig. 4) shows that the dark gray layer (V M2/3) is superimposed on an unlayered coarse sandy material (VI Cv) (Fig. 4E). Differences in the grain sizes between layer VI Cv and the unit V M2 and V M3 indicate that these layers derive from different sedimentation events. As the organic material in units VI Cv and V M2 does not form any coatings around the minerals a vertical relocation of the organic matter in the form of podsolization can be excluded (Phillips and FitzPatrick 1999; Wilson and Righi 2010). Regarding the sharp contrast in the organic content between unit VI Cv and V M1 as well as the topographic context, an interpretation as former topsoil material relocated at different events is more feasible and could explain the admixture of organic matter. Unit V M2 bears a higher content of silt material compared to the underlying V M1 (Fig. 4F and G). The homogenous distribution of minerogenic and organic material including charred organic matter could indicate that some of the organic material was already incorporated into this unit during the sedimentation process. Other features like mycorrhiza hyphae, roots, fecal pellets, and burrow features (Kooistra and Pulleman 2010) indicate that this horizon has been a surface for some time (Gerasimova and Lebedeva-Verba 2010). The boundary towards the unit IV M1 with coarser grain sizes is sharp (Fig. 4H). Although direct evidence by micromorphological features is missing, the observations about grain size, organic matter and bioturbation features are consistent with an interpretation of layer V M3/M2 and IV M3 as material relocated at different occasions along the slope as it is indicated by the topographic position and the inclination of the sediment units visible in the profile. The comparatively wide DE-distribution of the OSL measurements (Table 2) with positively skewed multimodal distribution indicates an insufficient resetting of the latent OSL signal before burial (i.e., incomplete exposition of the sediments to daylight) that could lead to an age overestimation. The calculated minimum-age-model therefore gives more weight to the DE-aliquots with weaker luminescence signals (i.e., better resetting of luminescence signal due to exposure to light) and results in an estimated minimum deposition age of 0.15 ± 0.04 ka (HUB-0749). Therefore, the deposition of this sandy layer should have occurred around 1860 ± 40 AD or some decade prior to that. Towards the stream, this colluvial sequence is covered by overbank deposits with relatively low

366 organic content in the basal part (II Go and III Go, Fig. 6, samples 6 and 7). The sequence of pollen spectra from the lowest colluvial layer and the alluvial sequence contain not only *Picea*, *Abies alba*, *Fagus*, *Alnus*, *Ulmus*, *Tila*, and *Carpinus betulus*, but also pollen indicative of a more open vegetation 369 caused by human activities, like *Secale cereale*, *Plantago lanceolate*, *Calluna vulgaris*, and *Rumex acetosella*-type. In comparison to the nearby profile 2, the deposition could be contemporary or postdating the biostratigraphical zone above 18 cm, representing the late Medieval to early Modern 372 period. While the subfossil driftwood in the alluvial sediments was determined as *Picea* and as *Picea/Abies* type, the charcoals in the sandy colluvial layers represent *Picea* and *Fagus*.

375 *Profile 4*

Profile 4 is located next to an isolated falls shaft feature (Fig. 2a) and shows a sequence with a mining heap on top of the weathered parent bedrock (gneiss) (Suppl. 5). Immediately below the mining 378 heap, remains of topsoil material (buried paleosol) with charcoal particles were found (II fAh horizon). ^{14}C analysis of some charcoal fragments yielded an age of 1292–1395 cal AD (Table 1) and provided a maximum age for the mining activities. The overburden mainly consists of gneiss 381 containing hammered pieces of quartz, probably originating from the locally occurring quartz veins.

Profile 5

384 This profile directly downslope of the glass kilns represents a sequence of at least three layers of silty material (M-Ah, II M, III M, IV M-Ah; Fig. 7a, samples 1–3) above a sandy substrate with weathered gneiss (V Bv). Given position of the profile on the slope below the plateau with the glass kilns and 387 indicated by the high organic content and the large number of chaotically admixed artifacts, these three layers are labeled as colluvial layers. Anyway, human activities like cleaning up of the plateau above may have contributed to the origin of these layers. The ceramic material (Fig. 7c) with high

collared rims (German: Hohe Kragenränder) and lids indicates a deposition of the material during or after the fourteenth century (Mechelk 1981; Geupel 1990). Fragments of glass crucibles, crushed quartz and glass slags (Fig. 7b) can be linked to the glass kilns situated directly above. Two samples of glass slags as well as one piece of crushed quartz were selected for geochemical analyses (see below).

Anthracologial spectra and macrobotanical remains from charcoal hearths

The sampled charcoal hearth sites indicate a high variability of the tree species used as fuel (Fig. 8). While the charcoal kilns in the west at the outlet of the valley are dominated by *Fagus* (hearths 2, 3, 6), a higher share of *Picea* is visible within the valley (hearths 1, 4, 5, 7, 10), *Abies* is mostly present in smaller quantities here as well. Uphill to the north, the share of *Abies* increases at the expense of *Picea* (hearths 8, 9). The wet-sieving of 3l of sediment from charcoal hearth 1 retrieved many thousands of charred needle fragments from *Picea* and *Abies*, therefore being in accordance with the anthracological spectrum, but no remains of any other plant material were found. As the dendrochronological dating of larger charcoal pieces failed, ^{14}C ages where obtained from charcoal hearth 1 and 2 (Table 1). Both ^{14}C-ages span rather long periods with 1470–1633 cal AD (MAMS-30567) for hearth 1 and 1666–1950 cal AD (MAMS-30568) for hearth 2, hence pointing to early modern to modern local charcoal production. Neither the ^{14}C-age obtained for the quartz mining nor the artefact spectrum at the kiln area indicates glass production later than the fourteenth century why the charcoal production is chronologically at least partly disconnected at the Ullersdorf site.

Geochemical analyses of glass slags and quartz from profile 5

The crushed quartz from profile 5 contains on average only a hundred ppm of Mg, Ca, P, and about 200 ppm Pb and Mn. In comparison to the glass slags, the quartz is pure and all elements detected in

414 the glass need to be additives because the glass shards are well preserved, homogeneous (Fig. 9a) and any randomly appearing alteration and secondary grown mineral was not observed. Totals are between 97.9 and 99.3 wt% for the glass slags which is indicative for a very low H_2O or CO_2 content.

417

Discussion

The onset of local human impact

420 The anthracological data (Fig. 8) could match the natural zonation of the forest cover in this topography showing a prevalence of *Picea abies*, a tree tolerant to wet (and cool) conditions (Leuschner and Ellenberg 2017), in charcoal hearths near the wet valley floor. Rising shares of *Abies* 423 *alba* could be observed on the hillslopes where this taxon can compete with *Fagus sylvatica*. The latter is dominant on the SW exposed hillslopes at the valley entrance, where more sunlight is available (Fig. 10, phase 1). The local presence of *Picea* on the valley floor is supported by charred 426 needle fragments in the upper layers of profile 2 as well as by the dominance of uncharred remains in the alluvial sediments in profile 3. A similar forest composition, strongly depending on local site conditions, could be reconstructed for the Medieval period in other uplands of central Europe (Kaiser 429 et al. 2019). Earlier studies (Geupel 1990) have suggested that settlement in the area may have started during the thirteenth century already, based on the toponym "Ullersdorf" and the typological assessment of some parts of the ceramic artifact assemblage. However, this phase becomes neither 432 visible in the pollen record in profile 2 nor in the artifacts observed in profile 5. Although our results do not contradict the assumption of an early rural settlement in this area, the possible location and duration of this settlement remains unresolved (Fig. 10, phase 2). Generally, the establishment of 435 early rural villages is corroborated by the nearby Hilmersdorf site (Geupel 1994). The isolated occurrence of pollen from *Secale cereale* and *Plantago lanceolata* pollen in profile 2 at 32 cm depth could be linked to the Roman Iron Age and is probably a result of long-distance input from the

438 settled foreland as already observed in other pollen sequences in the Erzgebirge such as in the mire Georgenfelder Hochmoor (Stebich 1995).

441 *Glass production phase*

Mining for quartz as well as glass production at this site have occurred during the fourteenth century based on the ^{14}C-age obtained below the mining heap in profile 4 and the dating of the diagnostic 444 artifacts mixed with glass slags and remains of glass melting containers in profile 5 downhill (Fig. 10, phase 3). The result of the geomagnetic survey shows three distinct anomalies on the nearby plateau that could match the layout and size of glass kilns. Compared with other sites in this region (Křivánek 447 1998, 2001), there is probably one central glass melting kiln (Fig. 2b, feature 1) with two auxiliary cooling kilns (Fig. 2b, features 2 and 3) that are smaller in size and show less pronounced geomagnetic amplitudes. Remarkably, quartz mining in the shaft near profile 4 predates any other 450 archeological evidence for mining in this part of the Erzgebirge so far. Mining technology in general flourished in the context of ore exploration in other parts of the Erzgebirge since the mid-twelfth century (Hemker et al. 2012; Hemker 2014, 2018; Schröder 2015) and may indicate the transfer of 453 mining technology to satisfy the need of the glass industry for quartz. Generally, the increasing demand for glass as a luxurious commodity led to the establishment of glass production sites in many European mountain ranges during the Late Medieval period (thirteenth/fourteenth centuries) (Černá 456 1996). These mountain environments could sufficiently meet the high demand for wood that was indispensable for the production of potash necessary for the glass making process and the fuel for glass kilns. In addition, commonly occurring quartz deposits, mostly found as veins in massive rock, 459 delivered the minerogenic raw material. Comparing the quartz and glass samples from profile 5, we observed that K_2O, Al_2O_3, CaO, and MgO must have been entered the material either deliberately or unintended during the manufacturing process or by taphonomic processes. Several authors (e.g., 462 Hartmann 1994; Wedepohl et al. 2009; Jackson and Smedley 2016) have investigated the

composition of medieval glass and the composition of beech and oak ashes but none of those glass compositions show such an elevated Al_2O_3 content as in the sample from Ullersdorf. While the contents of K_2O and CaO could vary by either using trunk or branch ash or ashes from both to save valuable trunk wood (Fig. 9B, Wedepohl et al. 2009), Al_2O_3 is always ≤1.5% in those glasses. Elevated contents of Al_2O_3 and K_2O in the glass could in theory point to the use of either white mica, like muscovite, or K-feldspar as Mining for quartz as well as glass production at this site have occurred during the fourteenth century based on the ^{14}C-age obtained below the mining heap in profile 4 and the dating of the diagnostic artifacts mixed with glass slags and remains of glass melting containers in profile 5 downhill (Fig. 10, phase 3). The result of the geomagnetic survey shows three distinct anomalies on the nearby plateau that could match the layout and size of glass kilns. Compared with other sites in this region (Křivánek 1998, 2001), there is probably one central glass melting kiln (Fig. 2b, feature 1) with two auxiliary cooling kilns (Fig. 2b, features 2 and 3) that are smaller in size and show less pronounced geomagnetic amplitudes. Remarkably, quartz mining in the shaft near profile 4 predates any other archeological evidence for mining in this part of the Erzgebirge so far. Mining technology in general flourished in the context of ore exploration in other parts of the Erzgebirge since the mid-twelfth century (Hemker et al. 2012; Hemker 2014, 2018; Schröder 2015) and may indicate the transfer of mining technology to satisfy the need of the glass industry for quartz. Generally, the increasing demand for glass as a luxurious commodity led to the establishment of glass production sites in many European mountain ranges during the Late Medieval period (13th / 14th centuries) (Černá 1996). These mountain environments could sufficiently meet the high demand for wood that was indispensable for the production of potash necessary for the glass making process and the fuel for glass kilns. In addition, commonly occurring quartz deposits, mostly found as veins in massive rock, delivered the minerogenic raw material. Comparing the quartz and glass samples from profile 5, we observed that K_2O, Al_2O_3, CaO, and MgO must have been entered the material either deliberately or unintended during the manufacturing process or by taphonomic processes. Several authors (e.g., Hartmann 1994; Wedepohl et al. 2009; Jackson and Smedley 2016) have investigated

the composition of medieval glass and the composition of beech and oak ashes but none of those glass compositions show such an elevated Al_2O_3 content as in the sample from Ullersdorf. While the contents of K_2O and CaO could vary by either using trunk or branch ash or ashes from both to save valuable trunk wood (Fig. 9b, Wedepohl et al. 2009), Al_2O_3 is always ≤ 1.5% in those glasses. Elevated contents of Al_2O_3 and K_2O in the glass could in theory point to the use of either white mica, like muscovite, or K-feldspar as quartz veins and are easily accessible. The possibility of using feldspar-rich sands with or without additives of lime and ashes for ancient glass production is described in Henderson (2013). Preliminary calculations suggest, that a mixture of K-Feldspar (Al_2O_3=18%, K_2O = 17%, SiO_2 = 65%; Deer et al. 2013) with e.g. beech ash from trunks and branches (K_2O = 20%, CaO = 45%, MgO = 12%, P_2O_5 = 10%; (Hartmann 1994)) and pure quartz in the ratio 3:1:4 could match the observed glass composition. However, as parallels from medieval glasses are absent so far, unintended alterations during production and post-depositional processes provide alternative explanations. Direct contact of the glass with ashes during processing could account for elevated K-contents as well as direct contact with the oven wall or crucibles. It would need a larger sample from a representative spectrum of glass artefacts from this site (that could only be obtained by larger and highly destructive excavation) to further substantiate the presence of Al_2O_3 and elevated K_2O-values. Several analyses have proven the wide use of lead in medieval glass production (Wedepohl et al. 2009; Mecking 2013) and have suggested a lead pollution of the nearby sediments (Seidel et al. 2013). Our results however do not indicate an addition of lead to the glass produced at the Ullersdorf site. The Pb-concentration instead reaches its maximum in those layers of profile 2 that postdate the operation of the glass kilns (Fig. 3). Besides ore mining, glass production became one of the most important early industries in the upper Erzgebirge region (Fig. 1a) and continued to supply the markets in Bohemia and Saxony and beyond from the late thirteenth century until modern times (Černá 1996, 2016; Kirsche 2014).

From the end of glass production to modern times

None of the dated nearby charcoal hearths or any colluvial/ alluvial layer dated in profiles 2 and 3 coincides with the local production of glass that started during the fourteenth century. Instead these features postdate this time period. These results are in accordance with the decline of arboreal pollen in profile 2, indicating deforestation and an increased influx of charcoal particles probably from the fifteenth century onwards (Fig. 10, phase 4). Based on the analysis of the regional DEM, this area stands out by a high density of charcoal hearth features. This development long after the onset of glass production is remarkable given the general conception of glass production to have caused massive, i.e., almost total local forest clearances (Bachmann 1996; Kirsche 2003). The rising concentration of the elements Pb and As in the layers above 18 cm in profile 2 is therefore not connected to the production of stained lead-glass. It is rather interpreted as a signal connected to the increased mining and smelting activities in the Marienberg mining district since at least the early sixteenth century (Wagenbreth 1990). This explains why the Pb-concentration develops parallel to the concentration of arsenic as characteristic element from ore processing. Comparable rises of Pb-concentration as proxy for intensified mining activities are known from other regions of the Erzgebirge (Tolksdorf et al. 2018, 2019). As shown by the stratigraphical position of the colluvial layer in profile 2 and the OSL-dated colluvial layers in profile 3, most of the local soil erosion seems to have occurred during the nineteenth century in the context of ongoing charcoal production (Fig. 10, phase 4). Following a forest dieback in this area in the 1980s the hilltops were successfully reforested, it is mainly spruce plantations that cover the area now (Sachsenforst 2017; Fig. 10, phase 5).

Glass production and mining activities: competing for resources?

It seems that later phases of charcoal production since the sixteenth century after the abandonment of the glass kilns have had a much greater impact on the local environment, causing deforestation, soil erosion as well as colluvial and alluvial sedimentation. It therefore needs careful discussion whether the environmental impact of glass production may have been exaggerated generally, perhaps due to the overweighted considerations of historical sources on wood shortages, as these may have been biased by competing interests (Radkau 1983; Schmidt 2002). In this light, the absence

of any later glass industry in this area could be explained by the rise of mining and smelting in the Erzgebirge since the early sixteenth century as driving factors of economic development, which was supported by the local authorities. Another close connection between glass production and mining activities becomes apparent on a technological level with the need to prospect, mine, and process local quartz resources. It implies that knowledge about these technologies must have been present in this area but did not result in any ore mining activities. Why did mining in this area start later in comparison with other parts of the Erzgebirge, although glass production requiring similar technology was present and mining flourished elsewhere? Other sites with metallurgical activities, such as the "Schwedengraben" 9 km north of the Ullersdorf site, were already in operation during the thirteenth/fourteenth century (Geupel 1984b, 1992). In respect of these divergent regional developments the influence of changing political structures on the industrial activities may have yet been underestimated compared to factors like technological abilities and resource availability.

Conclusions

The expected strong impact of a glass kiln site on the environment in a small catchment was studied by the application and combination of a broad set of methods. While evidence for settlement activities prior to the fourteenth century is rare, the operation of glass kilns together with the mining of quartz is evident at the Ullersdorf site during the fourteenth century. However, an environmental impact of this industry could not be identified in the on-site records, whereas strong implications of later charcoal production are evident based on charcoal hearths off-site. The rising occurrence of elements like lead or arsenic could conclusively be explained by the onset of mining activities in the nearby district of Marienberg. Against this backdrop, local charcoal production could have served the supply for metallurgical activities. Our results suggest that it may be problematic to presume a strong connection of charcoal production, soil erosion and the operation of glass kilns based on their spatial occurrence (Schneider et al. 2020) without sufficient chronological resolution to support synchronicity. Instead our case studies suggests that the role of glass kilns as consumers of wood may be overestimated based on contemporary sources, especially when compared in a diachronic

perspective to the impact caused by charcoal production in the context of mining. Future environmental studies in central European mountain areas should therefore not be limited to the direct impact of glass production but also include later phases as suitable reference and to address the question about competing industries and the political and economic development of the wider region.

Acknowledgements

Research was generously funded by the EU Interreg V program (ArchaeoMontan 2018). The State Forest Authority in Saxony (Sachsenforst) kindly gave permission for the fieldwork and the State Survey Office (Staatsbetrieb Geobasisinformation und Vermessung Sachsen, GeoSN) kindly provided LiDAR measurements for processing. We are indebted to V. Geupel, Y. Hoffmann, B. Kirschen, O. Huke and H. Zimack for advice during fieldwork and discussion of results. ICPOES and soil analyses were kindly performed by A. Guhl (TU Freiberg) and A. Körle (Humboldt-University Berlin), respectively. We especially thank four anonymous reviewers and the editor who helped to improve a previous version of this manuscript by detailed annotations.

Literature:

AG Boden AG (2005) Bodenkundliche Kartieranleitung. Hannover

Armbruster M, Abiy M, Feger KH (2003) The biogeochemistry of two forested catchments in the Black Forest and the eastern Ore Mountains (Germany). Biogeochemistry 65:341–368. doi: 10.1023/A:1026250209699

Bachmann HG (1996) Waldwirtschaft und Glashütten im Spessart. In: Jockenhövel A (ed) Bergbau, Verhüttung und Waldnutzung im Mittelalter. Auswirkungen auf Mensch und Umwelt. Vierteljahresschrift für Sozial- und Wirtschaftsgeschichte, Beiheft 212. Stuttgart, pp 181–188

Bebermeier W, Hoelzmann P, Meyer M, Schimpf S, Schütt B (2018) Lateglacial to Late Holocene landscape history derived from floodplain sediments in context to prehistoric settlement sites of the southern foreland of the Harz Mountains, Germany. Quaternary International 463:74–90. doi: 10.1016/j.quaint.2016.08.026

Berglund BW, Ralska-Jasiewiczowa M (1986) Pollen analysis and pollen diagramms. In: Berglund BE (ed) Handbook of Holocene Palaeoecology and Palaeohydrology. John Wiley & Sons, Chichester, pp 357–373

Beug H-J (2004) Leitfaden der Pollenbestimmung für Mitteleuropa und angrenzende Gebiete - mit 13 Tabellen. Pfeil, München

Billig G, Geupel V (1992) Entwicklung, Form und Datierungen der Siedlungen in der Kammregion des Erzgebirges. Siedlungsforschung Archäologie, Geschichte, Geographie 173–194

Bohdálková L, Bohdálek P, Břízová E, Pacherová, P., Kuběna, A. (2018) Atmospheric metal pollution records in the Kovářská Bog (Czech Republic) as an indicator of anthropogenic activities over the last three millennia. Science of The Total Environment 633:857–874. doi:10.1016/j.scitotenv.2018.03.142

Cappers RTJ, Bekker RM, Jans JEA (2012) Digitale zadenatlas van Nederland =: Digital seed atlas of the Netherlands, 2nd ed. Barkhuis Publ. [u.a.], Eelde

Černá E (2016) Středověké sklárny v severozápadních Čechách. Přínos archeologie k dějinám českého sklářství. Mittelalterliche Glashütten in Nordwestböhmen. Beitrag zur Geschichte des böhmischen Glashüttenwesens. Tiskárna, Most

Černá E (2014) Forschungsstand zu erzgebirgischen Glashütten. In: Černá E, Steppuhn P (eds) Glasarchäologie in Europa: Regionen - Produkte - Analysen ; Beiträge zum 5. Internationalen Symposium zur Erforschung mittelalterlicher und frühneuzeitlicher Glashütten Europas,

Seiffen/Erzgebirge 2012, 1. Aufl. Ústav Archeologické Památkové Péče Severozápadních Čech, Most, pp 13–26

Černá E (1996) Die hochmittelalterliche Glaserzeugung im östlichen Teil des Erzgebirges. In: Jockenhövel A (ed) Bergbau, Verhüttung und Waldnutzung im Mittelalter. Auswirkungen auf Mensch und Umwelt. Vierteljahresschrift für Sozial- und Wirtschaftsgeschichte, Beiheft 212. Stuttgart, pp 173–180

Černá E (1995) Eine mittelalterliche Glashütte bei Pockau im Erzgebirge. Arbeits- und Forschungsberichte zu sächsischen Bodendenkmalpflege 37:177–194

Chambers FM, van Geel B, van der Linden M (2011) Considerations for the preparation of peat samples for palynology,and for the counting of pollen and non-pollen palynomorphs. Mires and Peat 7:1–14

Cílová Z, Kučerová I, Knížová M, Trojek T (2015) Corrosion damage and chemical composition of Czech stained glass from 13th to 15th century. Glass Technology: European Journal of Glass Science and Technology Part A 56:153–162

Cílová Z, Woitsch J (2012) Potash – a key raw material of glass batch for Bohemian glasses from 14th–17th centuries? Journal of Archaeological Science 39:371–380. doi: 10.1016/j.jas.2011.09.023

Clark RL (1984) Effects of pollen preparation on charcoal. Pollen et Spores 26:559–576

Crkal J, Černá E (2009) Nové objevy v Krušných horách - zaniklé stredoveké sklárny na k. ú. Výsluní, okr. Chomutov. [Neue Entdeckungen im Erzgebirge - wüstgelassene mittelalterliche Glashütten im Katastergebiet Sonnenberg, Bezirk Chomutov]. Archaeologia historica 34:503–521

Deer WA, Howie RA, Zussman J (2013) An introduction to the rock-forming minerals, 3. edition. The Minerological Society, London

Deforce K, Boeren I, Adriaenssens S, Bastiaens J, De Keersmaeker L, Haneca K, Tys D, Vandekerkhove
636 K (2013) Selective woodland exploitation for charcoal production. A detailed analysis of charcoal kiln remains (ca. 1300-1900 AD) from Zoersel (northern Belgium). Journal of Archaeological Science 40: 681–689. doi: 10.1016/j.jas.2012.07.009

639 Durand A (2016) Medieval Southern Alpine Mountains: perceptions and interweaving diverse sources. In: Retamero F, Schellerup I, Davies A (eds) Making agro-pastoral landscapes in pre-industrial societies: choices, stability and change. Oxbow, Oxford, pp 251–270

642 Durcan JA, King GE, Duller GAT (2015) DRAC: Dose rate and age calculator for trapped charge dating. Quaternary Geochronology 28:54–61. doi: 10.1016/j.quageo.2015.03.012

Galbraith RF, Roberts RG, Laslett GM, Yoshida H, Olley JM (1999) Optical dating of single and multiple
645 grains of quartz from Jinmium Rock Shelter, northern Australia: Part I, experimental design and statistical models. Archaeometry 41:339–364. doi: 10.1111/j.1475-4754.1999.tb00987.x

Garnier E (2000) “The Coveted Tree”: the Industrial Threat to the Vosges Forest in the 16th and 18th
648 Centuries. In: Agnoletti M, Anderson S (eds) Forest History: International Studies on Socio-economic and Forest Ecosystem Change. CABI, Wallingford, pp 37–47

Gassiot Ballbè E, Clemente Conte I, Mazzucco N, Garcia Casas D, Obea Gómez L, Rodríguez Antón D
651 (2016) Surface surveying in high mountain areas, is it possible? Some methodological considerations. Quaternary International 402:35–45. doi: 10.1016/j.quaint.2015.09.103

Gerasimova M, Lebedeva-Verba M (2010) Topsoils-mollic, takyric and yermic horizons. In: Stoops G,
654 Marcelino V, Mees F (eds) Interpretation of Micromorphological Features of Soils and Regoliths. Elsevier, Amsterdam, pp 351–368

Geupel V (1995) Die vergessene Burg an den Nonnenfelsen. Erzgebirgische Heimatblätter 17:12–15

657 Geupel V (1994) Die Wüstung Hilmersbach in der Stadtflur Marienberg im Erzgebirge. Ausgrabungen und Funde 39: 27–31

Geupel V (1992) Die Ausgrabungen in der Wüstung “Schwedengraben” bei Niederlauterstein. Ein Haus des 13. Jahrhunderts. Arbeits- und Forschungsberichte zur sächsischen Bodendenkmalpflege 35: 163–176

Geupel V (1990) Ullersdorf - eine mittelalterliche Wüstung im mittleren Erzgebirge. Ausgrabungen und Funde 35: 40–45

Geupel V (1984a) Die mittelalterliche Wehranlage “Raubschloss” Liebenstein bei Olbernhau, Kr. Marienberg. Arbeits- und Forschungsberichte zur sächsischen Bodendenkmalpflege 27/28:289–307

Geupel V (1984b) Sondierungen in der Wüstung Schwedengraben bei Niederlauterstein, Kr. Marienberg. Ausgrabungen und Funde 29:30–37

Giesecke T, Bennett KD, Birks HJB, Bjune AE, Bozilova E, Feurdean A, Finsinger W, Froyd C, Pokorný P, Rösch M, Seppä H, Tonkov S, Valsecchi V, Wolters S (2011) The pace of Holocene vegetation change – testing for synchronous developments. Quaternary Science Reviews 30:2805–2814. doi: 10.1016/j.quascirev.2011.06.014

Gühne A (1983) Ein Glasschmelzplatz des 13. Jahrhunderts im Tharandter Wald, Gemarkung Grillenburg, Kr. Freital. Ausgrabungen und Funde 28:30–36

Hardy B, Dufey J (2015) Les aires de faulde en forêt wallone: repérage, morphologie et distribution spatiale. Forêt Nature 135:20–30

Hartmann G (1994) Late medieval glass manufacture in the Eichsfeld region (Thuringia, Germany). Chemie der Erde 54:103–128

Haslett J, Parnell A (2008) A simple monotone process with application to radiocarbon-dated depth chronologies. Journal of the Royal Statistical Society: Series C (Applied Statistics) 57:399–418. doi: 10.1111/j.1467-9876.2008.00623.x

681 Heiri O, Lotter AF, Lemcke G (2001) Loss on ignition as a method for estimating organic and carbonate content in sediments: reproducibility and comparability of results. Journal of Paleolimnology 25:101–110. doi: 10.1023/A:1008119611481

684 Hemker C (2014) Ausgewählte Funde des Jahres 2012 aus den hochmittelalterlichen Silbergruben von Dippoldiswalde und Niederpöbel. Ausgrabungen in Sachsens 4 Arbeits- und Forschungsberichte zur sächsischen Bodendenkmalpflege Beiheft 27: 363–374

687 Hemker C (2018) New insights on mining archaeology in the Erzgebirge (Ore Mountains). World of Mining - Surface & Underground 70:409–416

Hemker C, Hoffmann Y, Scholz V (2012) Silvermining at Dippoldiswalde during the medieval mining
690 period in Saxony. Acta rerum naturalium 12:79–98

Henderson J (2013) Ancient glass. Cambridge University Press, Cambridge ; New York

Hesse R (2010) LiDAR-derived Local Relief Models - a new tool for archaeological prospection.
693 Archaeological Prospection 17:67–72. doi: 10.1002/arp.374

Hildebrandt H, Heuser-Hildebrandt B, Wolters S (2007) Kulturlandschaftsgenetische und Bestandsgeschichtliche Untersuchungen anhand von Kohlholzspektren aus historischen
696 Meilerplätzen, Pollendiagrammen und archivalischen Quellen im Naturpark Pfälzerwald, Forstamt Johanniskreuz - Mainzer Geographische Studien, Sonderband 3. Mainz

Horák J, Klír T (2017) Pedogenesis, Pedochemistry and the Functional Structure of the Waldhufendorf
699 Field System of the Deserted Medieval Village Spindelbach, the Czech Republic. Interdisciplinaria Archaeologica - Natural Sciences in Archaeology VIII:43–57. doi: 10.24916/iansa.2017.1.4

Houfková P, Horák J, Pokorná A, Bešta T, Pravcová I, Novák J, Klír T (2019) The dynamics of a non-
702 forested stand in the Krušné Mts.: the effect of a short-lived medieval village on the local environment. Vegetation History and Archaeobotany 28: 607–621. doi: 10.1007/s00334-019-00718-5

Isenburg M (2014) LAStools - efficient LiDAR processing Software

Jackson CM, Smedley JW (2016) Theophilus and the use of beech ash as a glassmaking alkali. In: Martinón-Torres M, Rehren T (eds) Archaeology, History and Science. Routledge, New York, pp 117–130

Kaiser K, Hrubý P, Tolksdorf JF, Alper G, Herbig C, Kočár P, Petr L, Schulz L, Heinrich I (2019) Cut and covered: Subfossil trees in buried soils reflect medieval forest composition and exploitation of the central European uplands. Geoarchaeology 35: 42-62. doi: 10.1002/gea.21756

Kirsche A (2014) Zu den Wechselbeziehungen zwischen Glashütten, Waldwirtschaft und Bergbau im Erzgebirge. In: Černá E, Steppuhn P (eds) Glasarchäologie in Europa: Regionen - Produkte - Analysen ; Beiträge zum 5. Internationalen Symposium zur Erforschung mittelalterlicher und frühneuzeitlicher Glashütten Europas, Seiffen/Erzgebirge 2012, Ústav Archeologické Památkové Péče Severozápadních Čech, Most, pp 27–33

Kirsche A (2003) Glas und Holz: Vorindustrielle Glashütten im Erzgebirge und im Vogtland und ihr Einfluss auf die Seiffener Holzkunst. TU Dresden

Knapp H, Robin V, Kirleis W, Nelle O (2013) Woodland history in the upper Harz Mountains revealed by kiln site, soil sediment and peat charcoal analyses. Quaternary International 289: 88–100. doi: 10.1016/j.quaint.2012.03.040

Kooistra MJ, Pulleman MM (2010) Features Related to Faunal Activity. In: Stoops G, Marcelino V, Mees F (eds) Interpretation of Micromorphological Features of Soils and Regoliths. Elsevier, Amsterdam, pp 447-469

Kortzfleisch A von (2009) Räumliche Verteilung der Köhlerei in den Harzwäldern. In: Kortzfleisch A von, Feldmer P, Hermann-Reddersen-Stiftung (eds) Die Kunst der schwarzen Gesellen: Köhlerei im Harz, 2. Aufl. Papierflieger-Verl, Clausthal-Zellerfeld, pp 92–98

Křivánek R (1995) Geophysikalische Prospektion im Bereich der mittelalterlichen Glashütte Ullersdorf. Arbeits- und Forschungsberichte zur sächsischen Bodendenkmalpflege 37:199–203

Křivánek R (1998) Ergebnisse geophysikalischer Messungen von mittelalterlichen Glashütten im Erzgebirge. In: Osten-Woldenburg H von der (ed) Unsichtbares sichtbar machen: geophysikalische Prospektionsmethoden in der Archäologie. K. Theiss, Stuttgart, pp 147–159

Křivánek R (2001) Specifics and limitations of geophysical work on archaeological sites near industrial zones and coal mines in northwest Bohemia, Czech Republic. Archaeological Prospection 8:113–134. doi: 10.1002/1099-0763(200106)8:2<113::AID-ARP161>3.0.CO;2-N

Lange E, Christl A, Joosten H (2005) Ein Pollendiagramm aus der Mothäuser Heide am oberen Erzgebirge unweit des Grenzüberganges Reitzenhain. In: Sachenbacher P, Einicke R, Beier H-J (eds) Kirche und geistiges Leben im Prozess des mittelalterlichen Landesausbaus in Ostthüringen, Westsachsen. Beitr. Frühgesch. u. Mittelalter Ostthüringens 2. Langenweissbach, pp 153–169

Larsen A, Bork H-R, Fuelling A, Fuchs M, Larsen JR (2013) The processes and timing of sediment delivery from headwaters to the trunk stream of a Central European mountain gully catchment. Geomorphology 201:215–226. doi: 10.1016/j.geomorph.2013.06.022

Leuschner C, Ellenberg H (2017) Ecology of central European forests, Revised and extended version of the 6th German edition. Springer International Publishing AG, Cham

Ludemann T (2003) Large-scale reconstruction of ancient forest vegetation by anthracology - a contribution from the Black Forest. Phytocoenologia 33:645–666. doi: 10.1127/0340-269X/2003/0033-0645

Ludemann T (2011) Scanning the historical and scientific significance of charcoal production – local scale, high resolution kiln site anthracology at the landscape level. SAGVNTVM EXTRA 11:23–24

Lungershausen U, Heinrich C, Duttmann R, Gabler-Mieck R (2013) Turning human-nature interactions into 3D landscape scences: An approach to communicate geoarchaeological reseach. Kartographische Nachrichten Journal of Cartography and Geographic Information 63:269–275

Mannoni T, Giannichedda E (2011) Archeologia della produzione. Einaudi, Torino

Matschullat J, Ellminger F, Agdemir N, Cramer S, Ließmann W, Niehoff N (1997) Overbank sediment profiles evidence of early mining and smelting activities in the Harz mountains, Germany. Applied Geochemistry 12: 105–114. doi: 10.1016/S0883-2927(96)00068-6

Mechelk H (1981) Zur Frühgeschichte der Stadt Dresden und zur Herausbildung einer spätmittelalterlichen Keramikproduktion im sächsischen Elbgebiet aufgrund archäologischer Befunde. Akademie Verlag, Berlin

Mecking O (2013) Medieval lead glass in Central Europe. Archaeometry 55:640–662. doi: 10.1111/j.1475-4754.2012.00697.x

Milad M, Schaich H, Bürgi M, Konold W (2011) Climate change and nature conservation in Central European forests: A review of consequences, concepts and challenges. Forest Ecology and Management 261:829–843. doi: 10.1016/j.foreco.2010.10.038

Moore PD., Webb JA, Collinson ME (1991) Pollen analysis. Blackwell, Oxford

Murray A, Wintle A (2000) Luminescense dating of quartz using an improved single-aliquot regenerative dose protocol. Radiation Measurements 32:57–73. doi: 10.1016/S1350-4487(99)00253-X

Nalepka D, Walanus A (2003) Data processing in pollen analysis. Acta Palaeobotanica 43:125–134

Nelle O (2003) Woodland history of the last 500 years revealed by anthracological studies of charcoal kiln sites in the Bavarian Forest, Germany. Phytocoenologia 33:667–682. doi: 10.1127/0340-269X/2003/0033-0667

Östlund L, Zackrisson O, Strotz H (1998) Potash production in northern Sweden: History and ecological effects of a pre-industrial forest exploitation. Environment and History 4:345–358. doi: 10.3197/096734098779555592

Parnell A (2016) Bchron: Radiocarbon dating, age-depth modelling, relative sea level rate estimation, and non-parametric phase modelling. R package version 4.1. 1

Phillips DH, FitzPatrick EA (1999) Biological influences on the morphology and micromorphology of selected Podzols (Spodosols) and Cambisols (Inceptisols) from the eastern United States and north-east Scotland. Geoderma 90:327–364. doi:10.1016/S0016-7061(98)00121-9

Py-Saragaglia V, Cunill Artigas R, Métailié J-P, Ancel B, Baron S, Paradis-Grenouillet S, Lerigoleur É, Badache N, Barcet H, Galop D (2017) Late Holocene history of woodland dynamics and wood use in an ancient mining area of the Pyrenees (Ariège, France). Quaternary International 458:141-157. doi: 10.1016/j.quaint.2017.01.012

Raab A, Bonhage A, Schneider A, Raab T, Rösler H, Heußner KU, Hirsch F (2019) Spatial distribution of relict charcoal hearths in the former royal forest district Tauer (SE Brandenburg, Germany). Quaternary International 511:153–165. doi: 10.1016/j.quaint.2017.07.022

Raab A, Takla M, Raab T, Nicolay A, Schneider A, Rösler H, Heußner KU, Bönisch E (2015) Pre-industrial charcoal production in Lower Lusatia (Brandenburg, Germany): Detection and evaluation of a large charcoal-burning field by combining archaeological studies, GIS-based analyses of shaded-relief maps and dendrochronological age determination. Quaternary International 367:111–122. doi: 10.1016/j.quaint.2014.09.041

Raab T, Hirsch F, Ouimet W, Johnson KM, Dethier D, Raab A (2017) Architecture of relict charcoal hearths in northwestern Connecticut, USA. Geoarchaeology 32:502–510. doi: 10.1002/gea.21614

Radkau J (1983) Holzverknappung und Krisenbewußtsein im 18. Jahrhundert. Geschichte und Gesellschaft 9:513–543

Reimer P, Bard E, Bayliss A, Beck W (2013) IntCal13 and Marine13 Radiocarbon Age Calibration Curves 0–50,000 Years cal BP. Radiocarbon 55:1869–1887. doi: 10.2458/azu_js_rc.55.16947

Reinhardt-Imjela C, Imjela R, Bölscher J, Schulte A (2018) The impact of late medieval deforestation and 20th century forest decline on extreme flood magnitudes in the Ore Mountains (Southeastern Germany). Quaternary International 475:42–53. doi: 10.1016/j.quaint.2017.12.010

Richter U (2013) Die Besiedelung des Freiberger Raumes und die Entstehung der Stadt Freiberg. In: Hoffmann Y, Richter U (eds) Die Frühgeschichte Freibergs im überregionalen Vergleich Städtische Frühgeschichte - Bergbau - früher Hausbau. Mitteldeutscher Verlag, Halle, pp 13–31

Riols A (1992) Les verreries forestières et les charbonnières du Causse de l'Hortus (Hérault). Sources historiques et sites archéologiques. Bulletin de la Société Botanique de France Actualités Botaniques 139:609–616

Sachsenforst (2017) Exkursionsführer zur AFSV-Jahrestagung 2017. Standortswandel und Waldumbau im Oberen Erzgebirge. Staatsbetrieb Sachsenforst, Pirna

Schleich N (2006) Tiefenverteilung von Radionukliden in Fichtenwald- und Hochmoorböden. Dissertation Bergakademie Freiberg. Bergakademie Freiberg

Schlöffel M (2010) Die postglaziale Waldgeschichte der Lehmhaide. Rekonstruktion spät- und postglazialer Umweltbedingungen an einem Torfprofil aus dem Erzgebirge. Arbeits- und Forschungsberichte zu sächsischen Bodendenkmalpflege 51/52:9–27

Schmidt M, Mölder A, Schönfelder E, Engel F, Fortmann-Valtink W (2016) Charcoal kiln sites, associated landscape attributes and historic forest conditions: DTM-based investigations in Hesse (Germany). Forest Ecosystems 3:. doi: 10.1186/s40663-016-0067-6

Schmidt UE (2002) Der Wald in Deutschland im 18. und 19. Jahrhundert: das Problem der Ressourcenknappheit dargestellt am Beispiel der Waldressourcenknappheit in Deutschland im 18. und 19. Jahrhundert: eine historisch-politische Analyse. Conte/Forst, Saarbrücken

Schmitt A, Rodzik J, Zgłobicki W, Russok C, Dotterweich M, Bork HR (2006) Time and scale of gully erosion in the Jedliczny Dol gully system, south-east Poland. Catena 68:124–132. doi: 10.1016/j.catena.2006.04.001

Schneider A, Bonhage A, Raab A, Hirsch F, Raab T (2020) Large-scale mapping of anthropogenic relief features-legacies of past forest use in two historical charcoal production areas in Germany. Geoarchaeology doi: 10.1002/gea.21782

Schröder F (2015) Die montanarchäologischen Ausgrabungen in Niederpöbel (2011-2013)-Befunde und Ergebnisse. In: Smolnik R (ed) Archaeomontan 2015. Montanarchäologie im Erzgebirge. Arbeits- und Forschungsberichte zur sächsischen Bodendenkmalpflege Beiheft 30. Dresden, pp 23–166

Schulz L (2019) Visualization of forest development on a local scale. Master Thesis, TU Technical University Berlin. Institute for Landscape Architecture and Environmental Planning

Schweingruber FH (1990) Anatomie europäischer Hölzer. Haupt, Bern

Seidel J, Bebermeier W, Schütt B (2013) Historical Eco-Audit of Glassworks - a Case Study of the Eastern Ore Mountains. In: Raab T, Hirsch F, Raab A, Schopper F, Freytag K (eds) Arbeitskreis Geoarchäologie - Jahrestagung 2013. Tagungsband und Exkursionsführer. BTU Cottbus, Cottbus, p 37

Seifert-Eulen M (2016) Die Moore des Erzgebirges und seiner Nordabdachung. Vegetationsgeschichte ausgewählter Moore. Geoprofil 14:4–78

Slavíková L, Syrbe R-U, Slavík J, Berens A (2017) Local environmental NGO roles in biodiversity governance: a Czech-German comparison. GeoScape 11:1–15. doi: 10.1515/geosc-2017-0001

Stebich M (1995) Beiträge zur Vegetationsgeschichte des Georgenfelder Hochmoores. PhD dissertation University of Leipzig. Leipzig

Stockmarr J (1971) Tablets with spores used in absolute pollenanalysis. Pollen et Spores 615–621

Stoops G (2003) Guidelines for analysis and description of soil and regolith thin sections. Soil Science
843 Soc. of America, Madison

Swieder A (2019) Meilerrelikte als Teil der archäologischen Kulturlandschaft im östlichen Harz. Geopedology and Landscape Developement Research Series 8:43–72

846 Theuerkauf M, Couwenberg J, Kuparinen A, Liebscher V (2016) DISQOVER the Landcover - R based tools for quantitative vegetation reconstruction. Geophysical Research Abstracts 18:EGU2016-9933

Tolksdorf JF, Elburg R, Schröder F, Knapp H, Herbig C, Westphal T, Schneider B, Fülling A, Hemker C
849 (2015) Forest exploitation for charcoal production and timber since the 12th century in an intact medieval mining site in the Niederpöbel Valley (Erzgebirge, Eastern Germany). Journal of Archaeological Science:Reports 4:487–500. doi: 10.1016/j.jasrep.2015.10.018

852 Tolksdorf JF, Petr L, Schubert M, Herbig C, Kaltofen A, Matson S, Hemker C (2018) Palaeoenvironmental reconstruction in the mining town of Freiberg (Lkr. Mittelsachsen) in Saxony, from the 12th century onwards. Archäologisches Korrespondenzblatt 48:281–296

855 Tolksdorf JF, Schubert M, Schröder F, Petr L, Herbig C, Kočár P, Bertuch M, Hemker C (2019) Fortification, mining, and charcoal production: landscape history at the abandoned medieval settlement of Hohenwalde at the Faule Pfütze (Saxony, Eastern Ore Mountains). E&G Quaternary
858 Science Journal 67:73–84. doi: 10.5194/egqsj-67-73-2019

Tolksdorf JF, Schröder F, Petr L, Herbig C, Kaiser K, Kočár P, Fülling A, Heinrich S, Hönig H, Hemker C (2020) Evidence for Bronze Age and Medieval tin placer mining in the Erzgebirge mountains, Saxony
861 (Germany). Geoarchaeology 35:198–216. doi: 10.1002/gea.21763

van Geel B, Aptroot A, Mauquoy D (2006) Sub-fossil evidence for fungal hyperparasitism (Isthmospora spinosa on Meliola ellisii, on Calluna vulgaris) in a Holocene intermediate ombrotrophic
864 bog in northern-England. Review of Palaeobotany and Palynology 141:121–126. doi: 10.1016/j.revpalbo.2005.12.004

Wagenbreth O (ed) (1990) Bergbau im Erzgebirge: technische Denkmale und Geschichte, 1. Aufl. Dt. Verl. für Grundstoffindustrie, Leipzig

Wedepohl KH, Bergmann R, Kronz A (2009) Die Holzasche-Kalk-Blei-Gläser der Hütte am Füllenberg bei Altenbeken-Buke. Archäologie in Westfalen-Lippe 2009:207–213

Wedepohl KH, Simon K (2010) The chemical composition of medieval wood ash glass from Central Europe. Chemie der Erde - Geochemistry 70:89–97. doi: 10.1016/j.chemer.2009.12.006

Wedepohl KH, Simon K, Kronz A (2011) Data on 61 chemical elements for the characterization of three major glass compositions in late antiquity and the Middle Ages. Archaeometry 53:81–102. doi: 10.1111/j.1475-4754.2010.00536.x

Wilson MA, Righi D (2010) Spodic Materials. In: Stoops G, Marcelino V, Mees F (eds) Interpretation of Micromorphological Features of Soils and Regoliths. Elsevier, Amsterdam, pp 251–273

Figures:

Fig. 1 A: Erzgebirge / Krušné hory Mountain region with sites of glass production (compiled from Gühne 1983; Černá 1995, 1996; Křivánek 1998; Kirsche 2003; Crkal and Černá 2009); B: Topographic situation of study area with archaeological sites and palynological records (Lange et al. 2005; Schleich 2006; Schlöffel 2010; Seifert-Eulen 2016) covering the Mediaeval period; C: Density of charcoal hearth features (RCH) in the region of the Ullersdorf site. Inset 1: Digital elevation model (DEM, shaded relief) showing a concentration of hearth type 1 with a ridge; Inset 2: DEM with Concentration of hearths type 2 constructed as platforms on slope.

Fig. 2: A: Archaeological features with sampled profiles and charcoal hearths at Ullersdorf site. B: Results of a 0.5 m grid geomagnetic survey.

Fig. 3: Stratigraphy, sedimentology and geochemistry of profile 2 located in a peat on a stream terrace (see Fig. 2A).

Fig. 4: Left: Scan of thin sections: Right: A: microcharcoal in peat layer (III Hr); B: microcharcoal in overlaying layer (II Gr-fM); C: microaggregates (brown) and dislocated fragmented organic material (arrows); D: aggregate of *Meliola ellisii* spores; E: unlayered coarse sandy material in VI Cv; F: sharp boundary between V M2 (finer material) and V M3 (coarser material); G: fine material in V M2; H: sharp boundary between IV M1 (coarse material) and V M2 (fine material)

Fig. 5: Palynology and chronology of profile 2.

Fig. 6: Stratigraphy, palynology and chronology of profile 3 located in the stream floodplain.

Fig. 7A: Stratigraphy and sedimentology of profile 5 immediately downhill of the glass kilns; 7B: Glass slags from colluvial layers M1-M3; 7C: Selected ceramic fragments including remains from glass melting containers (1-2), broad rim (3), high collar rim (4), and lid fragment (5).

Fig. 8: Anthracological spectra from the charcoal hearths at the Ullersdorf site with topographic situation and ^{14}C ages.

Fig. 9A: Mounted glass sample from Ullersdorf site with SEM-EDX measurement spots (see Table 3); B: CaO/K_2O plot with results from Ullersdorf, reference samples from the medieval glass production site Moldava I site in Bohemia (Černá 2016), typical ranges of different glass types from literature (Wedepohl and Simon 2010; Wedepohl et al. 2011), and glass from experimental production according to different formulas (Cílová and Woitsch 2012).

Fig. 10: Scenes from idealized 3D reconstruction of the landscape dynamics at the Ullersdorf site. Phase 1: Forest vegetation undisturbed by any local human impact, early 12th century; Phase 2: Tentative land-use associated with rural colonization in this area, mid-13th century; Phase 3: Glass production during the 14th century AD; Phase 4: After the glass production has been abandoned

charcoal production is still very active and causes local clearances and soil erosion up to the 19th century; Phase 5: Today the area is completely reforested by managed stands of mainly *Picea*.

Tab. 1: Results of ^{14}C-analyses

Tab. 2: Result of OSL-analyses

Tab. 3: Results of SEM-EDX analyses of glass slag and quartz

Supplements

Suppl. 1: A: Aerial view on study area, B: Example of ridges typical for charcoal hearth as seen on the ground; C: Photo of profile 2; D: Photo of profile 3; E: Photo of profile 5

Suppl. 2: Soil data

Suppl. 3: Geochemical data from profile 2

Suppl. 4: Comparison of biostratigraphical units between Ullersdorf profile 2 and the corresponding units in the time-depth-models of the Mothäuser Heide record. Changes in the abundance or decline of specific taxa are indicated as trends by arrows.

Suppl. 5: Stratigraphy of profile 4 at the mining heap feature; inset 8B: Samples from the mining heap containing the overburden material (gneiss) and quartz of lesser purity left behind.

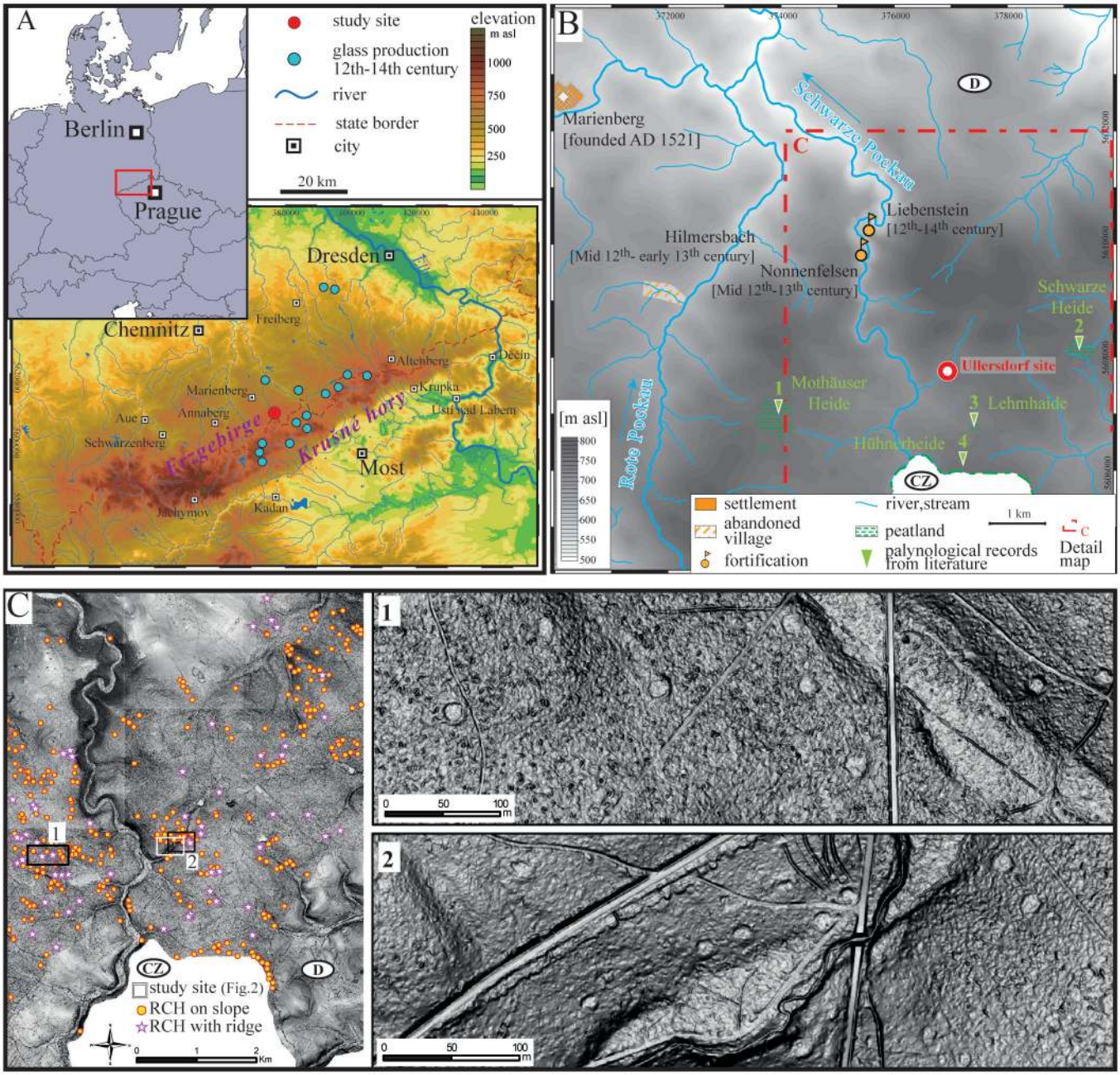

Fig. 1 A: Erzgebirge / Krušné hory Mountain region with sites of glass production (compiled from Gühne 1983; Černá 1995, 1996; Křivánek 1998; Kirsche 2003; Crkal and Černá 2009); B: Topographic situation of study area with archaeological sites and palynological records (Lange et al. 2005; Schleich 2006; Schlöffel 2010; Seifert-Eulen 2016) covering the Mediaeval period; C: Density of charcoal hearth features (RCH) in the region of the Ullersdorf site. Inset 1: Digital elevation model (DEM, shaded relief) showing a concentration of hearth type 1 with a ridge; Inset 2: DEM with concentration of hearths type 2 constructed as platforms on slope.

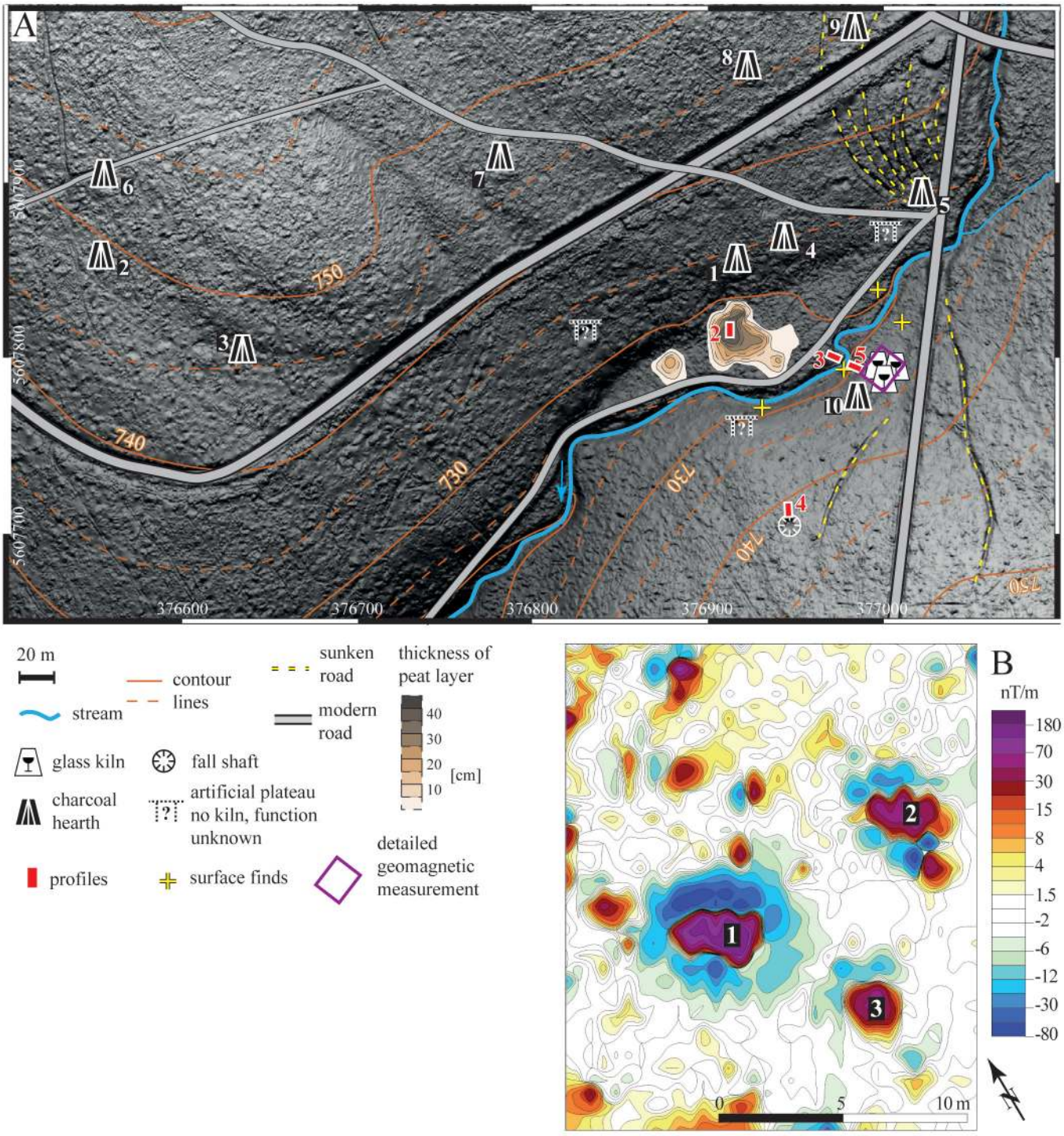

Fig. 2: A: Archaeological features with sampled profiles and charcoal hearths at Ullersdorf site.
B: Results of a 0.5 m grid geomagnetic survey.

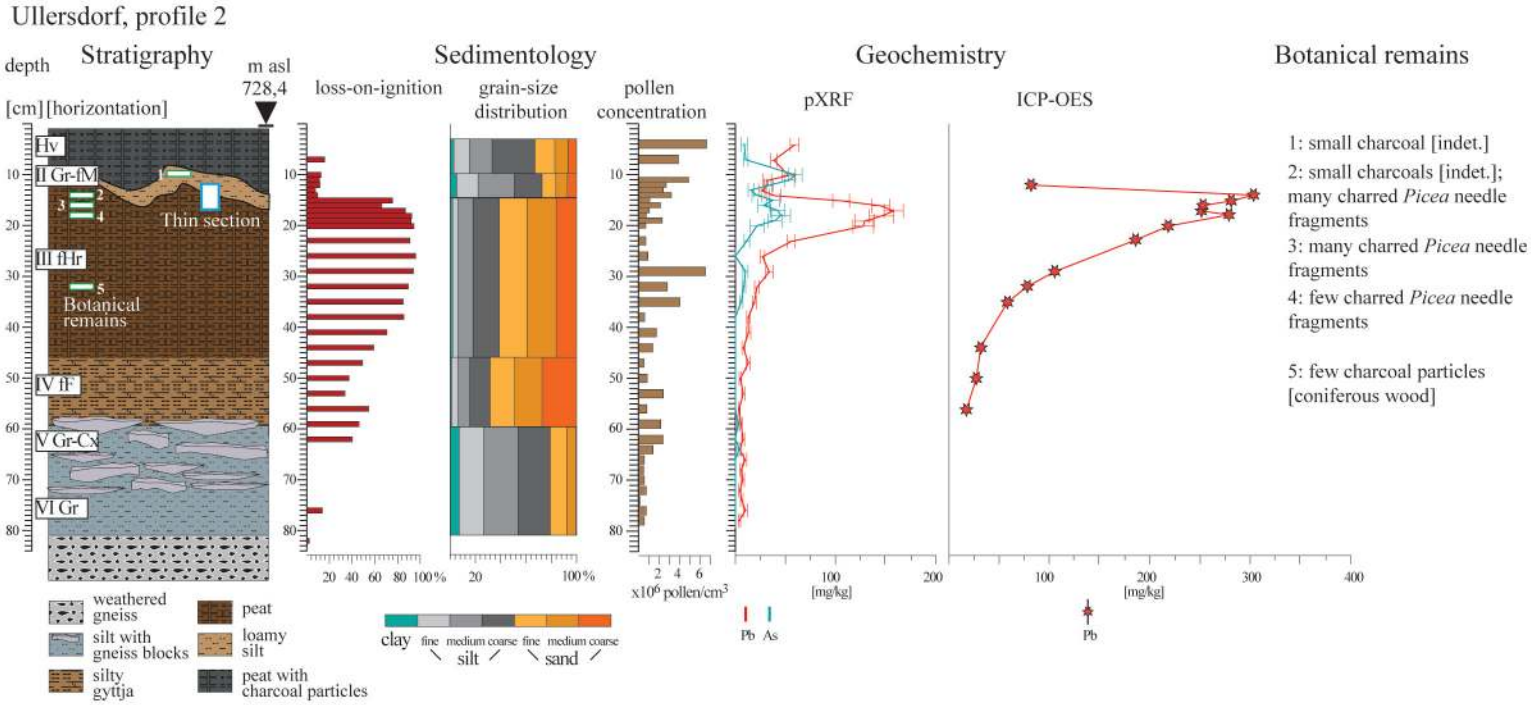

Fig. 3: Stratigraphy, sedimentology and geochemistry of profile 2 located in a peat on a stream terrace (see Fig. 2A).

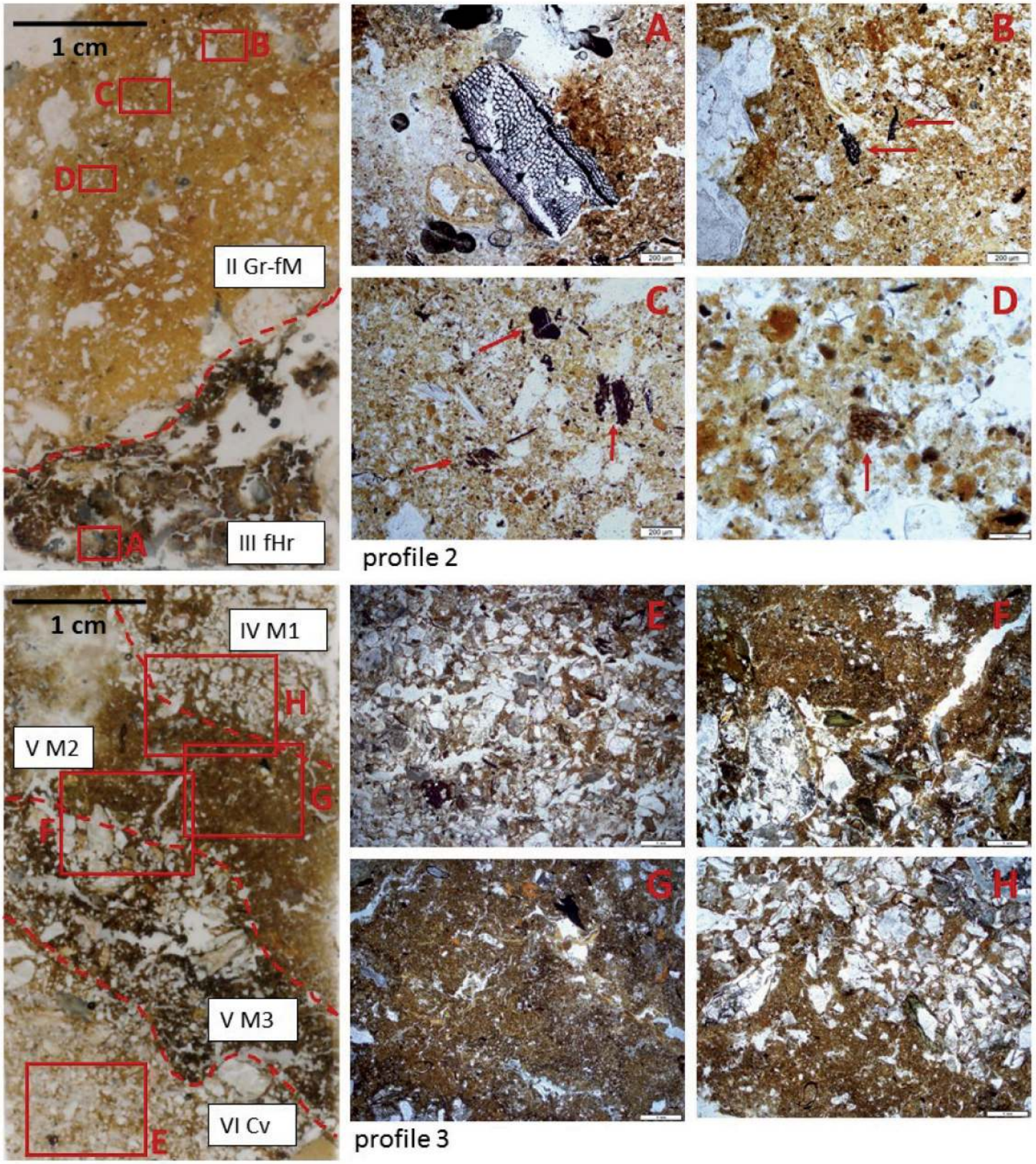

Fig. 4: Left: Scan of thin sections: Right: A: microcharcoal in peat layer (III Hr); B: microcharcoal in overlaying layer (II Gr-fM); C: microaggregates (brown) and dislocated fragmented organic material (arrows); D: aggregate of Meliola ellisii spores; E: unlayered coarse sandy material in VI Cv; F: sharp boundary between V M2 (finer material) and V M3 (coarser material); G: fine material in V M2; H: sharp boundary between IV M1 (coarse material) and V M2 (fine material)

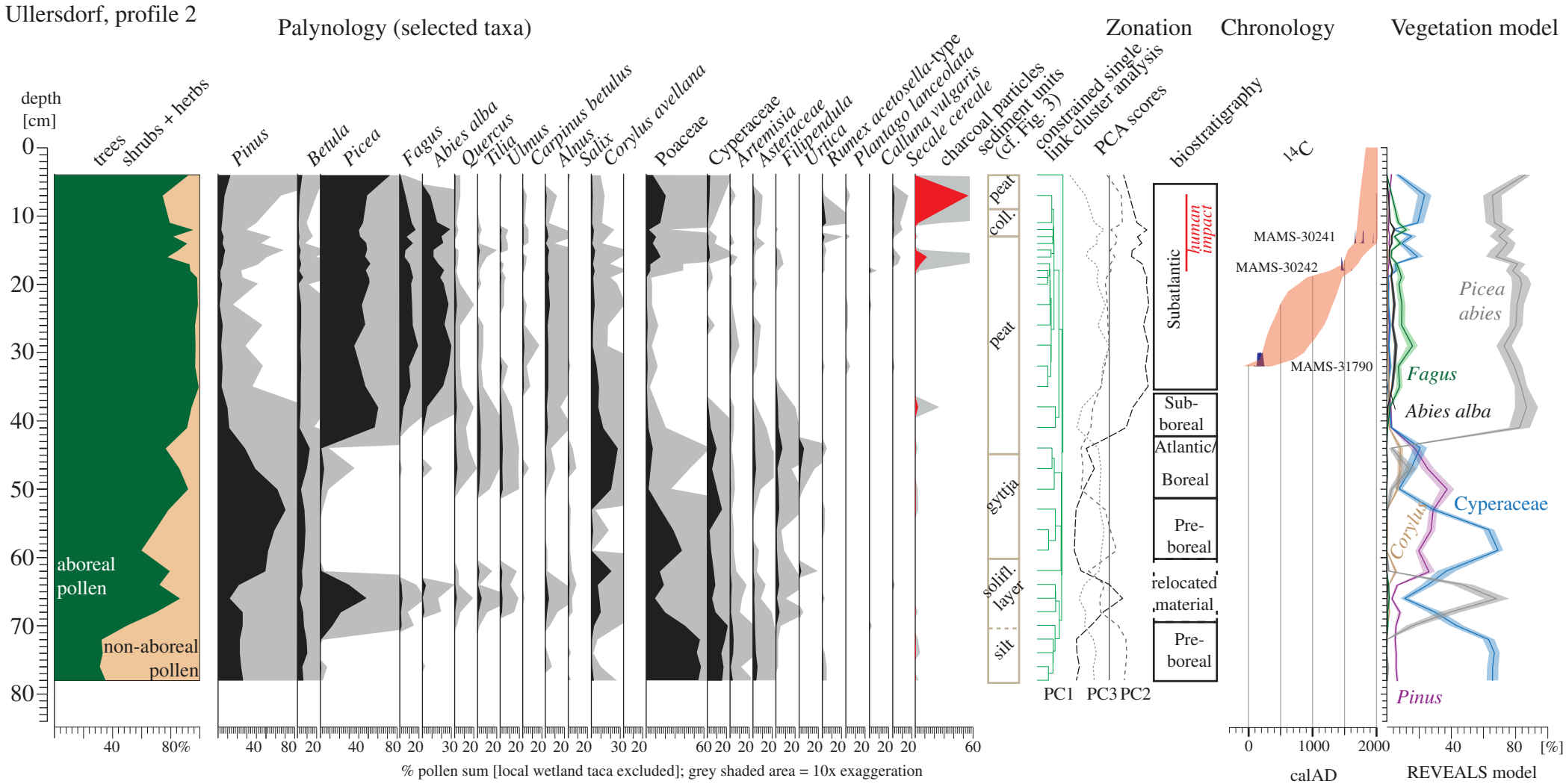

Fig. 5: Palynology and chronology of profile 2.

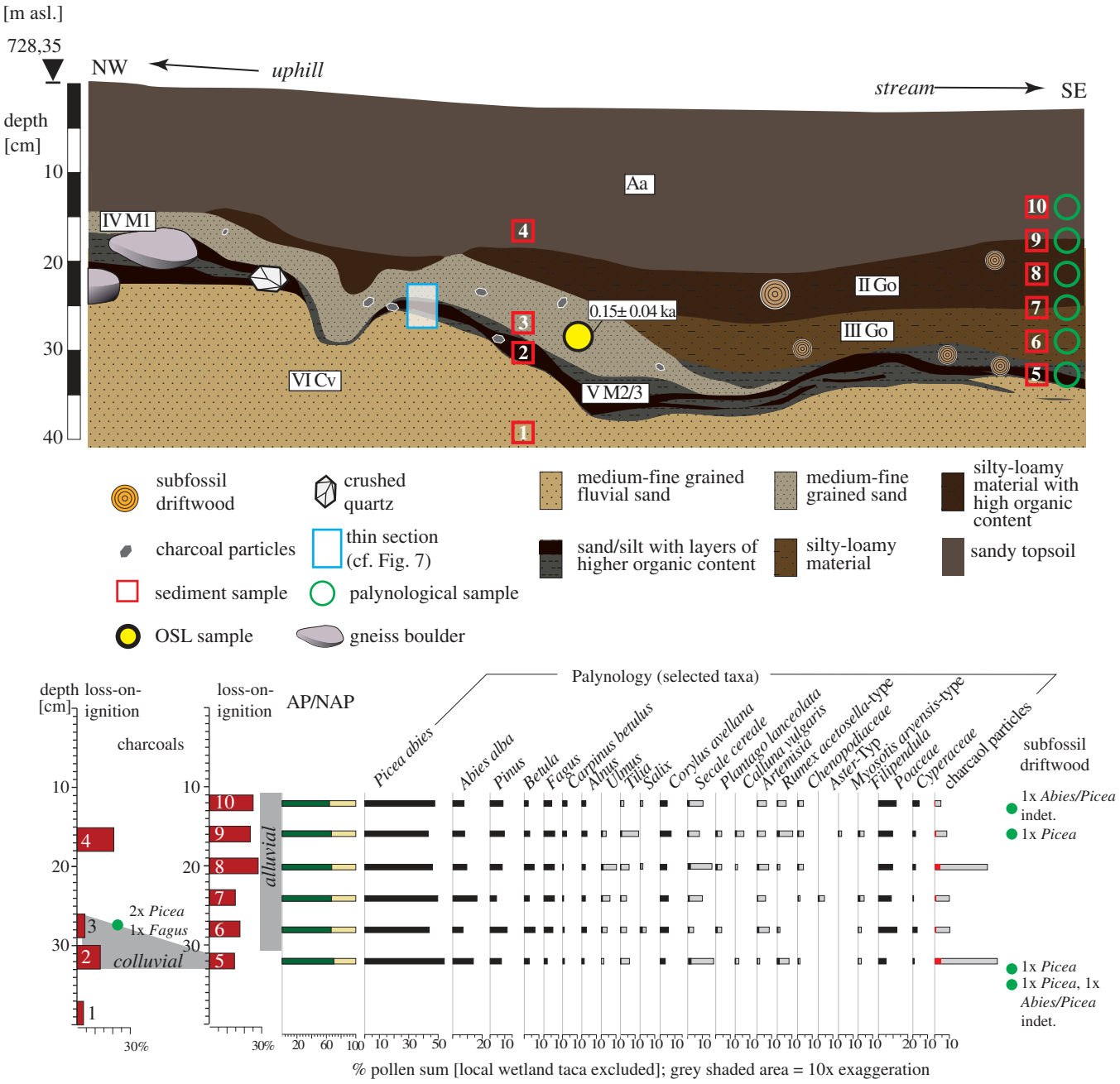

Fig. 6: Stratigraphy, palynology and chronology of profile 3 located in the stream floodplain.

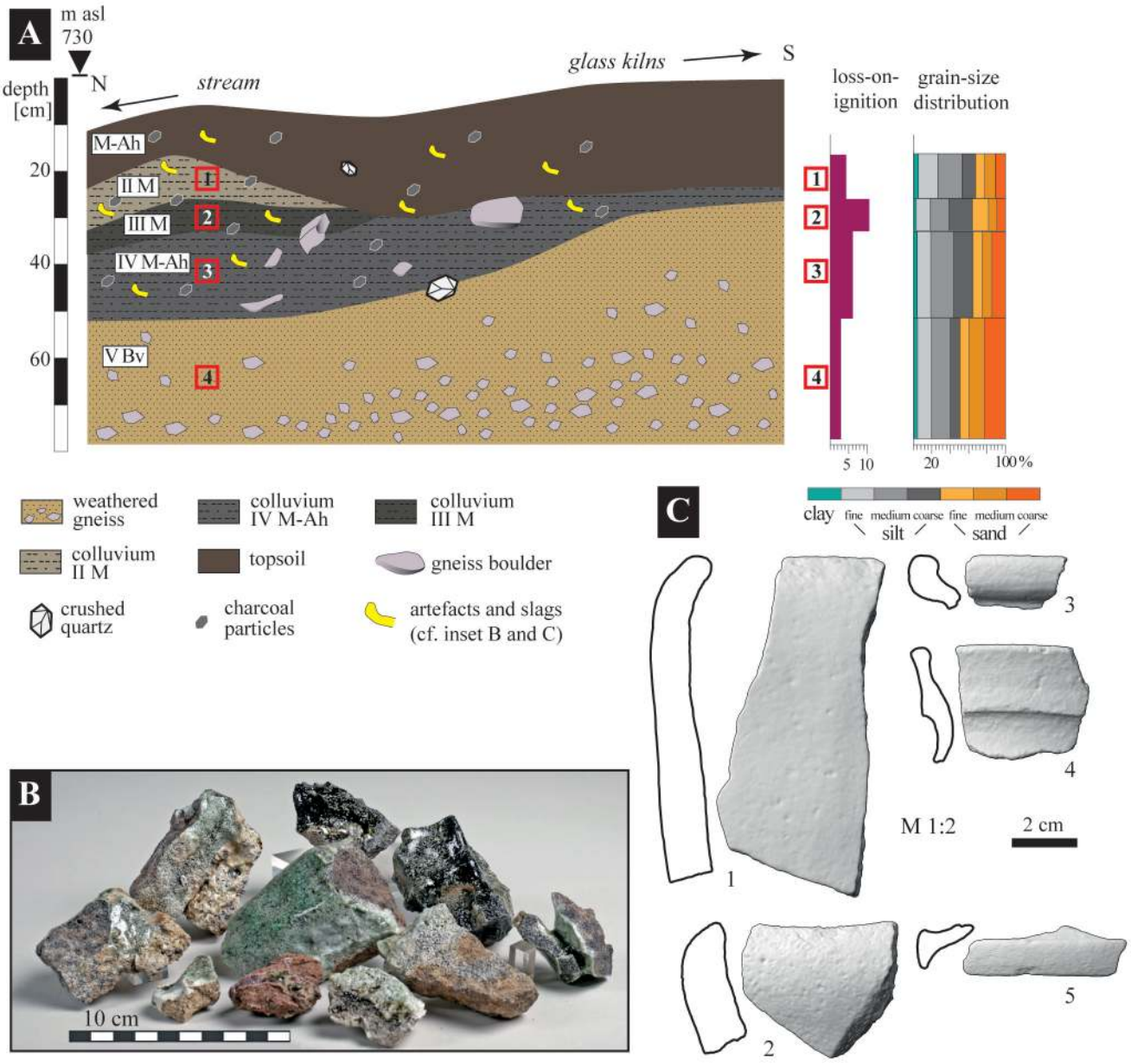

Fig. 7A: Stratigraphy and sedimentology of profile 5 immediately downhill of the glass kilns; 7B: Glass slags from colluvial layers M1-M3; 7C: Selected ceramic fragments including remains from glass melting containers (1-2), broad rim (3), high collar rim (4), and lid fragment (5).

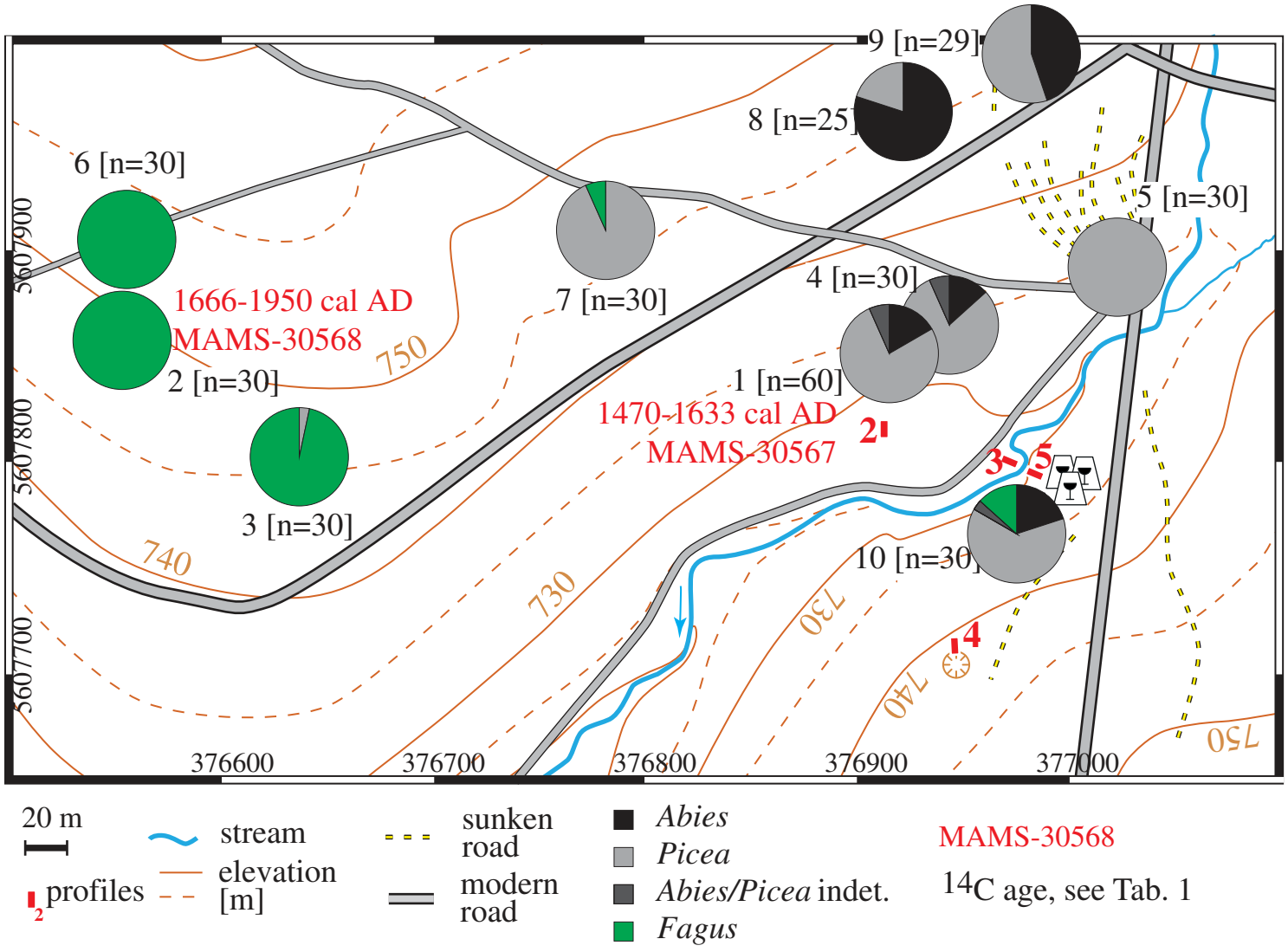

Fig. 8: Anthracological spectra from the charcoal hearths at the Ullersdorf site with topographic situation and ^{14}C ages.

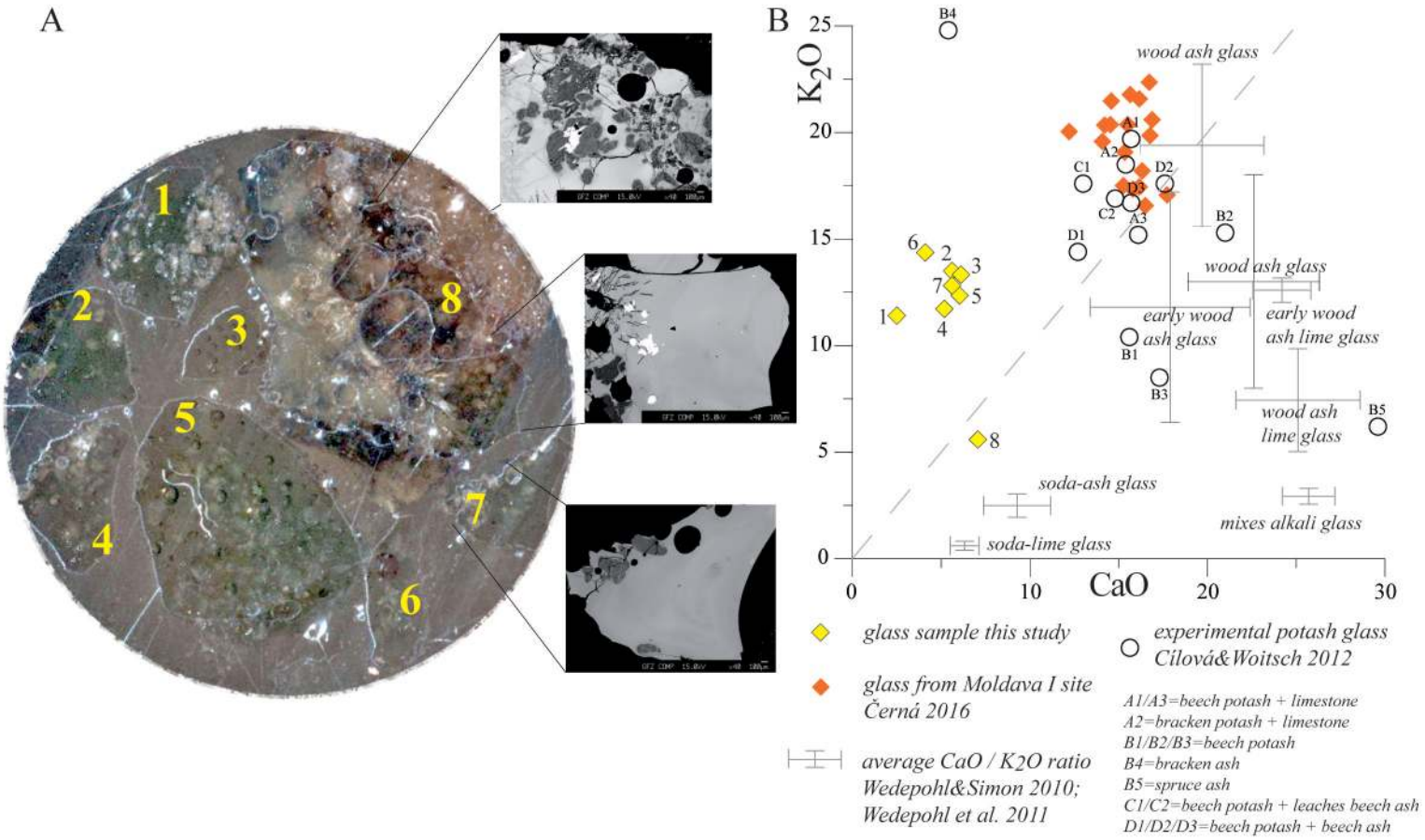

Fig. 9A: Mounted glass sample from Ullersdorf site with SEM-EDX measurement spots (see Table 3); B: CaO/K_2O plot with results from Ullersdorf, reference samples from the medieval glass production site Moldava I site in Bohemia (Černá 2016), typical ranges of different glass types from literature (Wedepohl and Simon 2010; Wedepohl et al. 2011), and glass from experimental production according to different formulas (Cílová and Woitsch 2012).

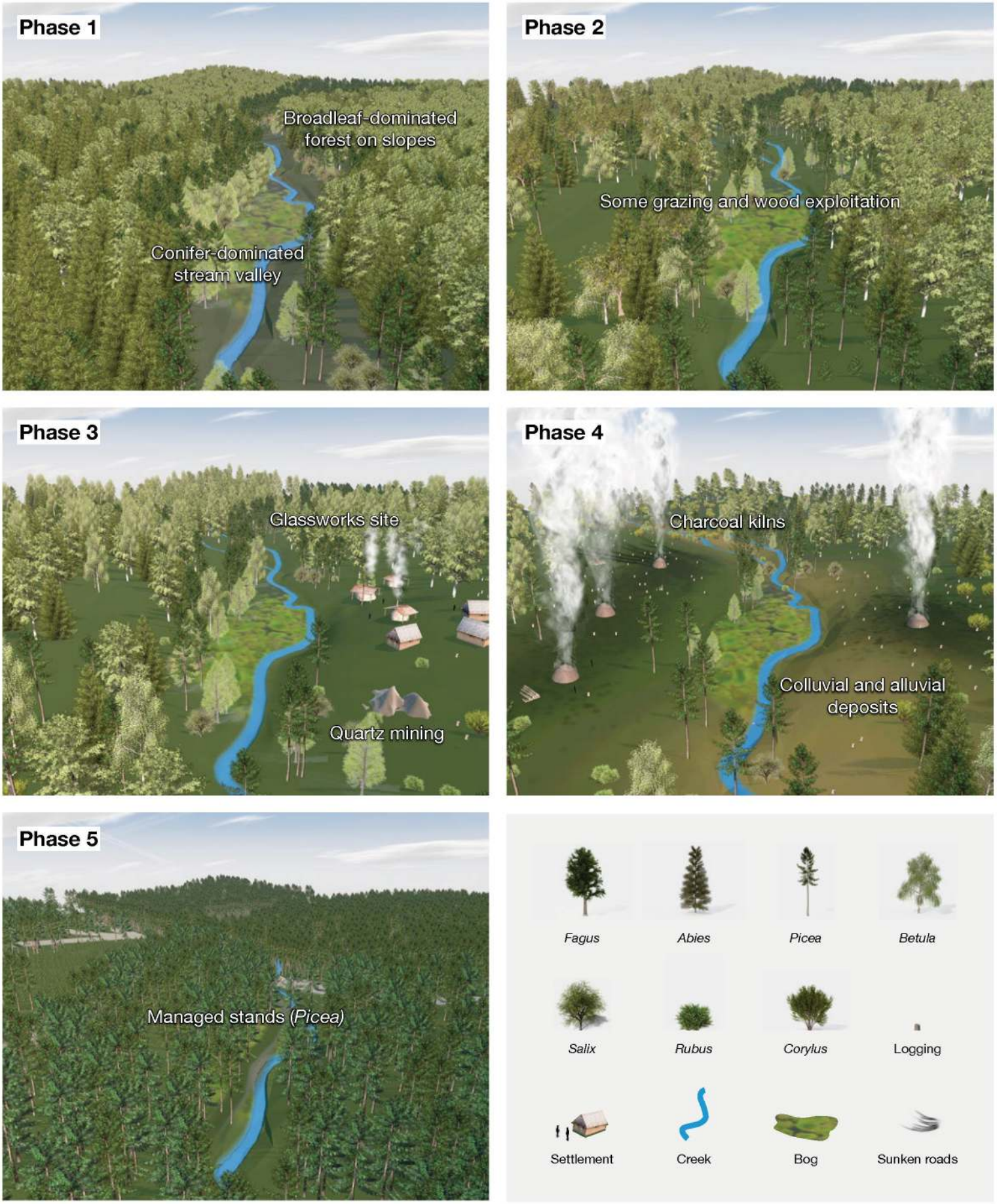

Fig. 10: Scenes from idealized 3D reconstruction of the landscape dynamics at the Ullersdorf site. Phase 1: Forest vegetation undisturbed by any local human impact, early 12th century; Phase 2: Tentative land-use associated with rural colonization in this area, mid-13th century; Phase 3: Glass production during the 14th century AD; Phase 4: After the glass production has been abandoned charcoal production is still very active and causes local clearances and soil erosion up to the 19th century; Phase 5: Today the area is completely reforested by managed stands of mainly Picea.

LabNo.	profile and depth below surface	material	^{14}C	^{14}C (calibrated; IntCal13, 1σ)	^{14}C (calibrated ; IntCal13, 2σ)	$\delta^{13}C$ (AMS)	comment
			[BP]	[cal AD]	[cal AD]	[‰]	
MAMS-30241	profile 2, 14 cm depth	charred needles (*Picea abies*)	207 ± 17	1661-1950	1652-1950	-23.8	pollen profile
MAMS-30242	profile 2, 18 cm depth	charred needles (*Picea abies*)	408 ± 20	1446-1472	1439-1613	-40.5	pollen profile
MAMS-31406	profile 4, 45-51 cm depth	charcoal particle indet.	626 ± 19	1299-1390	1292-1395	-40.5	below mining heap
MAMS-30567	charcoal hearth 1, 10 cm depth	charred needles (*Abies alba* and *Picea abies*)	345 ± 18	1490-1628	1470-1633	27.7	charcoal hearth
MAMS-30568	charcoal hearth 2, 10 cm depth	charred twig (*Fagus sylvatica*)	171 ± 18	1670-1944	1666-1950	-29.7	charcoal hearth
MAMS-31790	profile 2, 32 cm depth	charcoal particle indet.	1831 ± 24	138-216	93-244	-29.6	pollen profile

Table 1

Lab-No.	HUB-0749
Profile No.; depth below surface [cm]; elevation [m a.s.l.]; H_2O content [mass %]; processed grain size fraction [µm]	profile 3; 25 cm depth; 728 m a.s.l.; 40 ± 10 % H_2O; 90-200 µm
Measurement equipment	Risø TI/OSL-DA-15C7C unit; $^{90}Sr/^{90}Y$ β-ray emission 0.085 Gy/s
D_E measurement parameters	preheat: 200°C; 4 mm stencil; recycling ratio: 0.9-1.1; recuperation < 10%; OSL IR depletion ratio >0.9
Content of ^{238}U / ^{232}Th / ^{40}K in the sediment [ppm]	^{238}U: 4.31 ± 0.19 ppm; ^{232}Th: 10.05 ± 0.52 ppm; ^{40}K: 2.84 ± 0.05 ppm
D_0 Dose rate [Gy/ka]	3.29 ± 0.19 Gy/ka
D_E Equivalent dose	0.49± 0.13 Gy (Minimum Age Model (MAM) according Galbraith et al. (1999) was applied. An overdispersion of sigma b = 0.2 was set within the MAM)
OSL age	**0.15 ± 0.04 ka**

Technical report and results used to calculate the OSL age

measurement area (see fig. 10)	Al_2O	K_2O	FeO	Na_2O	CaO	SiO_2	MgO	TiO_2	MnO	P_2O_5	SO_3	PbO	Ag_2O
1	5.32	11.41	1.86	0.23	2.50	76.23	0.63	0.20	0.13	0.12	*0.00*	*0.01*	*0.00*
2	5.85	13.51	1.83	0.33	5.61	69.23	1.17	0.37	0.27	0.18	*0.00*	*0.01*	*0.00*
3	4.61	13.34	1.54	0.33	6.12	70.29	1.12	0.25	0.32	0.19	*0.01*	*0.00*	*0.00*
4	6.45	11.73	1.66	0.25	5.18	72.04	1.07	0.40	0.25	0.15	*0.00*	*0.00*	*0.00*
5	6.26	12.35	1.51	0.27	6.04	70.13	1.23	0.36	0.28	0.17	*0.00*	*0.00*	*0.00*
6	4.86	14.37	1.58	0.36	4.10	72.49	0.79	0.26	0.20	0.10	*0.00*	*0.00*	*0.00*
7	4.88	12.82	1.44	0.33	5.61	70.49	1.13	0.30	0.28	0.15	*0.01*	*0.00*	*0.00*
8	7.17	5.59	2.27	0.07	7.07	73.68	1.13	0.49	0.30	0.18	*0.01*	*0.01*	*0.00*
crushed quartz from profile 5	*0.01*	*0.00*	*0.00*	*0.00*	*0.00*	99.50	*0.01*	*0.00*	*0.02*	*0.01*	*0.00*	*0.02*	*0.00*

Median values of mass % of oxides from repeated measurements with JXA 8500F EPMA. Values in italics are below detection limit. Natural volcanic glass from Lipari was used as cross reference material.

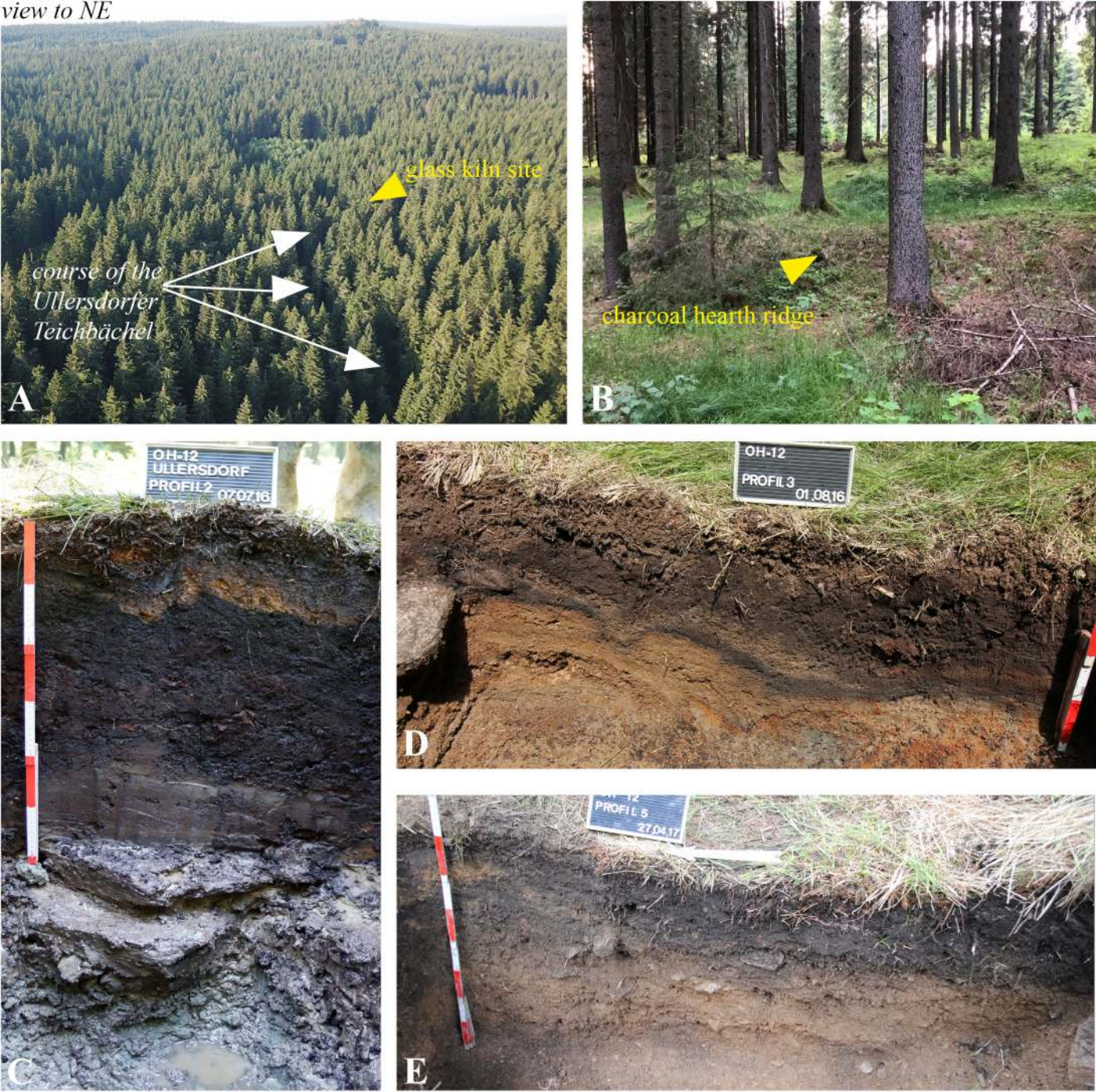
view to NE
glass kiln site
course of the
Ullersdorfer
Teichbächel
A
charcoal hearth ridge
B
OH-12
ULLERSDORF
PROFIL 2
07.07.16
C
OH-12
PROFIL 3
01.08.16
D
PROFIL 5
27.04.17
E

Profile ID	Sample ID	Sampling depth	Sediment facies	Soil horizon	Soil horizon	Colour	Grain-size composition, main fractions			Textural class	Grain-size composition, single fractions							Loss-on-ignition
							Clay <0.002 mm	Silt <0.063 mm	Sand <2 mm		Clay <0.002 mm	Fine silt <0.0063 mm	Medium silt <0.02	Coarse silt <0.063 mm	Fine sand <0.2	Medium sand <0.63	Coarse sand <2 mm	
		(cm)		(KA5)[1]	(FAO)[2]		(%)	(%)	(%)	(KA5)	(%)	(%)	(%)	(%)	(%)	(%)	(%)	(%)
2	KG-121	5-7	Peat	Hv	He	black	1,7	65,2	33,1	Us	3,0	12,5	17,8	33,6	16,0	10,7	6,4	55,5
2	KG-122	7-14	Colluvial (silt)	II Gr-fM	2Crb	yellow brown	2,7	70,0	27,3	Us	5,0	17,2	28,5	22,0	10,9	9,3	7,1	12,0
2	KG-123	36-40	Peat	III fHr	3Heb	black	3,7	37,3	59,0	Su3	1,9	5,1	11,0	21,2	22,3	22,4	16,1	88,9
2	KG-124	56-60	Lacustrine (organic gyttja)	IV fF	4Lrb	dark greyish brown	4,7	30,4	64,9	Su3	1,4	4,9	9,7	15,8	19,3	21,6	27,4	80,8
2	KG-125	60-75	Solifluction layer (stones, silty matrix)	V Gr-Cx	5Cr	olive grey	5,7	73,1	21,2	Us	7,2	19,5	27,2	24,9	14,1	6,5	0,6	10,4
2	-	75-80	Cover bed (gravel), weathered gneiss	VI Gr	6Cr	grey	-	-	-	-	-	-	-	-	-	-	-	-
3	KG-12	15	Fluvial (loam)	Go-aAa	Ah/Cl	black	-	-	-	-	-	-	-	-	-	-	-	-
3	KG-35	20	Fluvial (loam)	II Go-faAa	2Ah/Cl	dark brown	-	-	-	-	-	-	-	-	-	-	-	-
3	KG-33	28	Fluvial (loam)	III Go-faAa	3Ah/Cl	brown	-	-	-	-	-	-	-	-	-	-	-	-
3	KG-30	25-30	Colluvial (sand)	IV Go-M1	4Cl	light grey brown	1,7	43,2	55,1	Su4	3,8	9,3	13,9	20,0	18,4	22,5	12,1	4,5
3	KG-29	30-35	Colluvial (silt)	V Go-M2	5Cl	dark brown	2,7	54,0	43,3	Us	2,7	8,9	14,6	30,5	31,9	9,4	2,0	13,2
3	KG-28	40	Fluvial (sand)	VI Go	6Cl	reddish brown	3,7	44,0	52,3	Su4	5,4	11,0	16,0	17,0	19,7	19,4	11,5	3,8
4	-	0-5	Mining rubble (gravel)	yAh	Ahu	black	-	-	-	-	-	-	-	-	-	-	-	-
4	-	5-40	Mining rubble (gravel and stones)	ylC	Cu	dark grey	-	-	-	-	-	-	-	-	-	-	-	-
4	-	40-45	Palaeosol (formed from silty cover bed)	II fAh	2Ahb	grey with black dots	-	-	-	-	-	-	-	-	-	-	-	-
4	-	45-80	Weathered gneiss	III Bv, III ICv	3Bw, 3C	reddish brown	-	-	-	-	-	-	-	-	-	-	-	-
5	-	0-10	Colluvial (silt)	M-Ah	Ah	black	-	-	-	-	-	-	-	-	-	-	-	-
5	KG-129	10-18	Colluvial (silt)	II M	2Ahb	brown-grey	3,7	64,0	32,3	Us	5,6	20,3	27,0	14,8	10,1	11,4	10,8	4,4
5	KG-130	18-25	Colluvial (silt)	III M	3Ahb	dark grey-brown	4,7	59,9	35,4	Us	3,4	14,3	20,8	26,1	17,2	9,2	9,0	10,6
5	KG-131	25-32	Colluvial (silt)	IV M-Ah	4Ahb	light grey-brown	5,7	59,2	35,1	Us	3,8	15,3	24,6	21,2	9,4	11,2	14,5	6,1
5	KG-132	32-62	Cover bed (sand), weathered gneiss	V Bv	5Bw	brown	6,7	46,7	46,6	Su4	3,9	15,4	20,8	10,5	9,5	17,0	22,9	2,9

[1]Ad-hoc-AG Boden, 2005. Bodenkundliche Kartieranleitung (KA5), 5th edition. Schweizerbart, Hannover.
[2]FAO, 2006. Guidelines for Soil Description, 4th edition. FAO, Rome.

XRF measurement profile 2 [Innov X Delta device equipped with a 4W Rh tube and 25mm silicon drift detector (SSD) in soil analysis mode], values below detection limit=ND

Depth (cm)	Al	Al +/-	Si	Si +/-	P	P +/-	S	S +/-	Cl	Cl +/-	K	K +/-	Ca	Ca +/-	Ti	Ti +/-	Mn	Mn +/-	Fe	Fe +/-	Cu	Cu +/-	Zn	Zn +/-	As	As +/-	Rb	Rb +/-	Sr	Sr +/-	Y	Y +/-	Zr	Zr +/-	Nb	Nb +/-	Mo	Mo +/-	Pb	Pb +/-	Th	Th +/-	U	U +/-	LE	LE +/-	LOI (4h, 550°C) [%]
4,00	3,70	0,46	9,96	0,37	0,68	0,07	1,57	0,07	ND		0,86	0,04	6,43	0,19	0,53	0,07	0,16	0,02	4,29	0,14	0,03	0,01	0,04	0,00	0,01	0,00	0,02	0,00	ND		0,03	0,00	0,01	0,00	0,01	0,00	0,06	0,00	0,09	0,01	0,01	0,00	71,53	0,89	ND
7,00	7,11	0,45	35,31	0,67	0,27	0,06	0,33	0,04	ND		2,85	0,07	0,35	0,04	1,00	0,08	ND		2,39	0,06	ND		0,01	0,00	0,01	0,00	0,02	0,00	0,01	0,00	ND		0,04	0,00	0,01	0,00	0,00	0,00	0,04	0,00	0,03	0,01	0,00	0,00	50,22	0,89	15,79
10,00	10,13	0,65	67,46	0,60	0,55	0,14	0,58	0,09	ND		7,98	0,15	0,29	0,10	2,52	0,21	0,14	0,03	9,68	0,20	ND		0,02	0,01	0,06	0,01	0,05	0,00	0,02	0,00	ND		0,08	0,01	0,01	0,00	ND		0,05	0,01	0,11	0,03	0,01	0,00	0,25	0,02	13,02
11,00	8,97	0,55	55,27	0,74	0,49	0,10	0,21	0,05	ND		5,42	0,11	ND		1,65	0,14	ND		7,29	0,15	ND		ND		0,05	0,00	0,03	0,00	0,01	0,00	ND		0,07	0,01	0,01	0,00	ND		0,03	0,00	0,07	0,02	ND		20,41	0,86	11,29
12,00	8,57	0,52	44,81	0,76	0,40	0,08	0,14	0,04	ND		3,99	0,09	ND		1,25	0,11	ND		7,90	0,16	ND		0,01	0,00	0,03	0,00	0,04	0,00	0,01	0,00	ND		0,05	0,01	0,01	0,00	0,01	0,00	0,03	0,00	0,06	0,01	0,01	0,00	32,69	1,02	12,04
13,00	7,45	0,49	41,24	0,76	0,27	0,06	0,11	0,04	ND		3,64	0,09	ND		0,78	0,08	ND		7,59	0,16	ND		ND		0,02	0,00	0,04	0,00	0,01	0,00	ND		0,03	0,01	0,01	0,00	0,01	0,00	0,03	0,00	0,04	0,01	ND		38,73	1,04	7,86
14,00	10,42	0,60	65,48	0,54	0,51	0,12	0,31	0,07	ND		7,50	0,13	ND		1,79	0,16	ND		13,43	0,21	ND		0,02	0,01	0,02	0,00	0,05	0,00	0,02	0,00	ND		0,07	0,01	0,02	0,00	ND		0,04	0,01	0,10	0,02	ND		0,21	0,01	9,95
15,00	6,62	0,67	33,73	0,96	1,20	0,13	2,47	0,11	ND		3,04	0,11	1,21	0,07	1,10	0,13	ND		10,68	0,32	ND		0,02	0,01	0,04	0,01	0,01	0,00	0,01	0,00	ND		ND		0,01	0,00	0,01	0,00	0,11	0,01	0,07	0,02	ND		39,67	1,55	75,89
16,00	6,34	0,64	25,43	0,84	0,99	0,11	2,48	0,11	ND		1,99	0,08	1,24	0,07	0,74	0,10	ND		5,04	0,18	ND		0,03	0,01	0,03	0,01	0,01	0,00	0,01	0,00	ND		0,03	0,01	0,01	0,00	0,01	0,00	0,15	0,01	0,11	0,02	0,01	0,00	55,36	1,36	66,59
17,00	7,59	0,71	29,64	0,92	1,17	0,13	2,79	0,13	ND		3,05	0,11	1,42	0,08	1,15	0,14	ND		3,34	0,13	ND		0,05	0,01	0,04	0,01	0,01	0,00	0,01	0,00	ND		0,03	0,01	0,01	0,00	ND		0,16	0,01	ND		0,01	0,00	49,53	1,44	87,52
18,00	9,95	0,94	34,75	1,15	1,71	0,21	4,66	0,22	ND		3,75	0,16	2,97	0,15	1,62	0,21	ND		5,30	0,22	ND		0,03	0,01	0,05	0,01	0,01	0,00	0,01	0,00	ND		ND		ND		ND		0,15	0,01	ND		0,01	0,00	35,03	1,86	92,80
19,00	7,64	0,79	15,30	0,69	0,66	0,10	3,02	0,15	ND		1,31	0,07	2,11	0,10	0,79	0,11	ND		5,67	0,24	ND		ND		0,04	0,01	0,01	0,00	0,01	0,00	ND		ND		ND		ND		0,13	0,01	0,10	0,02	0,01	0,00	63,23	1,46	92,22
20,00	9,46	0,94	16,23	0,78	1,17	0,15	3,64	0,19	ND		1,47	0,09	2,87	0,14	0,99	0,14	ND		4,36	0,20	ND		0,02	0,00	0,02	0,01	0,01	0,00	0,01	0,00	ND		ND		ND		ND		0,13	0,01	0,07	0,02	0,01	0,00	59,54	1,68	94,80
23,00	4,94	0,54	9,76	0,39	0,24	0,06	1,61	0,07	ND		0,79	0,04	1,34	0,05	0,27	0,05	ND		1,62	0,06	ND		0,01	0,00	0,01	0,00	0,00	0,00	0,01	0,00	0,02	0,00	0,02	0,00	0,01	0,00	0,06	0,00	0,07	0,01	0,01	0,00	79,22	0,77	91,34
26,00	3,86	0,44	6,86	0,27	0,18	0,04	0,86	0,04	0,76	0,14	0,45	0,02	0,90	0,03	0,17	0,04	ND		0,88	0,03	ND		ND		ND		0,00	0,00	0,01	0,00	0,02	0,00	0,01	0,00	0,01	0,00	0,03	0,00	0,07	0,01	0,01	0,00	84,92	0,58	96,35
29,00	6,28	0,68	6,69	0,36	0,24	0,07	1,93	0,09	ND		0,69	0,04	2,91	0,11	0,29	0,06	ND		2,07	0,09	ND		0,01	0,00	0,01	0,00	0,00	0,00	0,01	0,00	0,03	0,00	0,02	0,00	0,01	0,00	0,01	0,00	0,03	0,00	0,11	0,01	0,01	0,00	78,63	0,94	94,5
32,00	4,29	0,50	8,34	0,34	0,15	0,05	1,58	0,07	0,75	0,17	0,58	0,03	2,33	0,08	0,30	0,06	ND		1,15	0,05	ND		0,01	0,00	0,01	0,00	0,01	0,00	0,03	0,00	ND		0,01	0,00	0,01	0,00	0,02	0,00	0,09	0,01	0,01	0,00	80,33	0,73	89,82
35,00	4,50	0,45	9,96	0,34	0,21	0,05	1,66	0,06	ND		0,79	0,03	2,75	0,08	0,45	0,06	ND		1,50	0,05	ND		0,02	0,00	0,01	0,00	0,01	0,00	0,02	0,00	0,03	0,00	0,02	0,00	0,01	0,00	0,02	0,00	0,06	0,01	0,01	0,00	78,00	0,69	85,55
38,00	3,85	0,43	6,03	0,25	ND		1,57	0,06	ND		0,57	0,03	3,12	0,09	0,21	0,04	ND		1,13	0,04	0,02	0,01	0,02	0,00	ND		0,01	0,00	0,02	0,00	0,02	0,00	0,02	0,00	0,01	0,00	0,01	0,00	0,01	0,00	0,07	0,01	0,01	0,00	83,30	0,59	85,96
41,00	7,81	0,60	17,60	0,57	0,36	0,07	2,27	0,09	ND		1,94	0,07	3,77	0,12	0,88	0,10	ND		2,52	0,09	ND		0,03	0,00	ND		0,02	0,00	0,02	0,00	0,05	0,01	0,04	0,01	0,01	0,00	0,01	0,00	0,08	0,01	0,01	0,00	62,56	1,08	70,78
44,00	6,79	0,48	19,62	0,50	0,36	0,05	1,54	0,06	ND		2,05	0,06	2,00	0,06	0,69	0,07	ND		1,41	0,05	ND		0,02	0,00	ND		0,02	0,00	0,02	0,00	0,02	0,00	0,03	0,00	0,01	0,00	0,00	0,00	0,01	0,00	0,04	0,01	0,01	0,00	65,35	0,83	59,36
47,00	9,08	0,53	27,43	0,64	0,33	0,06	1,21	0,06	ND		2,80	0,08	1,72	0,06	0,75	0,08	ND		2,56	0,08	ND		0,04	0,00	ND		0,03	0,00	0,02	0,00	0,07	0,01	0,03	0,01	0,01	0,00	0,00	0,00	0,01	0,00	0,05	0,01	0,01	0,00	53,86	0,99	49,14
50,00	8,36	0,41	24,66	0,48	0,33	0,04	0,40	0,03	ND		1,95	0,05	0,49	0,03	0,53	0,05	ND		2,35	0,06	ND		0,02	0,00	ND		0,02	0,00	0,01	0,00	0,04	0,00	0,02	0,00	0,00	0,00	ND		0,01	0,00	ND		0,00	0,00	60,81	0,71	37,56
53,00	8,12	0,54	20,79	0,56	0,34	0,06	0,48	0,04	ND		1,38	0,05	0,57	0,03	0,36	0,06	ND		1,58	0,05	ND		0,02	0,00	ND		0,02	0,00	0,01	0,00	0,04	0,00	0,03	0,00	0,00	0,00	ND		0,01	0,00	0,03	0,01	0,01	0,00	66,22	0,87	33,91
56,00	5,96	0,41	13,13	0,34	0,16	0,03	0,72	0,03	ND		0,92	0,03	0,61	0,02	0,19	0,04	ND		0,99	0,03	ND		0,01	0,00	ND		0,01	0,00	0,01	0,00	0,05	0,00	0,02	0,00	ND		ND		0,00	0,00	ND		0,00	0,00	77,21	0,58	54,79
59,00	7,00	0,42	15,14	0,37	0,29	0,04	1,52	0,05	ND		1,14	0,03	1,02	0,03	0,36	0,05	ND		1,43	0,04	0,02	0,00	0,02	0,00	0,00	0,00	0,01	0,00	0,06	0,00	0,03	0,00	0,00	0,00	ND		0,01	0,00	0,03	0,01	0,01	0,00	71,89	0,65	46,55
62,00	6,74	0,43	24,20	0,54	0,16	0,05	1,12	0,05	ND		2,13	0,06	2,56	0,07	0,56	0,06	ND		2,18	0,06	ND		0,02	0,00	ND		0,02	0,00	0,02	0,00	0,05	0,00	0,03	0,00	0,01	0,00	0,00	0,00	0,01	0,00	0,04	0,01	0,01	0,00	80,14	0,84	40,29
64,00	8,31	0,46	25,07	0,55	0,18	0,05	1,04	0,05	ND		2,25	0,06	2,15	0,06	0,72	0,07	ND		2,41	0,07	ND		0,02	0,00	0,00	0,00	0,02	0,00	0,02	0,00	0,07	0,00	0,03	0,00	0,01	0,00	0,00	0,00	0,00	0,00	0,03	0,01	0,01	0,00	57,64	0,86	ND
66,00	8,98	0,46	26,09	0,55	0,14	0,04	0,90	0,04	ND		2,45	0,06	1,56	0,05	0,67	0,07	ND		2,66	0,07	0,02	0,01	0,01	0,00	ND		0,03	0,00	0,02	0,00	0,06	0,00	0,03	0,00	0,01	0,00	ND		0,01	0,00	0,04	0,01	0,01	0,00	56,32	0,85	ND
68,00	7,87	0,40	21,92	0,44	ND		0,47	0,03	ND		1,77	0,04	0,63	0,03	0,52	0,05	0,02	0,01	1,91	0,05	ND		0,01	0,00	ND		0,02	0,00	0,01	0,00	0,09	0,00	0,03	0,00	0,00	0,00	ND		0,01	0,00	0,02	0,01	0,00	0,00	64,69	0,68	ND
70,00	10,23	0,46	31,93	0,59	ND		0,12	0,03	ND		2,86	0,06	0,28	0,03	0,60	0,06	ND		3,47	0,08	ND		0,02	0,00	ND		0,03	0,00	0,02	0,00	0,03	0,00	0,04	0,00	0,00	0,00	ND		0,01	0,00	0,04	0,01	0,01	0,00	50,31	0,85	ND
72,00	9,13	0,43	28,40	0,54	ND		0,09	0,02	ND		2,68	0,06	0,16	0,03	0,59	0,06	ND		3,03	0,07	ND		0,03	0,00	ND		0,03	0,00	0,01	0,00	0,03	0,00	0,03	0,00	0,00	0,00	ND		0,00	0,00	ND		0,00	0,00	55,79	0,78	ND
74,00	10,05	0,43	31,40	0,55	ND		ND		ND		2,81	0,06	0,21	0,03	0,63	0,06	0,03	0,01	3,19	0,07	ND		0,03	0,00	ND		0,03	0,00	0,01	0,00	0,03	0,00	0,03	0,00	0,01	0,00	ND		0,01	0,00	ND		ND		51,52	0,79	ND
76,00	11,31	0,48	37,76	0,65	ND		0,10	0,03	ND		3,78	0,08	0,25	0,04	0,82	0,08	ND		4,34	0,10	ND		0,05	0,00	ND		0,03	0,00	0,02	0,00	0,05	0,01	0,05	0,00	0,01	0,00	0,00	0,00	0,01	0,00	0,05	0,01	0,01	0,00	41,38	0,91	13,61
78,00	8,91	0,41	31,01	0,54	ND		ND		ND		3,10	0,06	0,10	0,03	0,72	0,06	0,03	0,01	2,61	0,06	ND		0,02	0,00	ND		0,02	0,00	0,01	0,00	0,01	0,00	0,04	0,00	0,00	0,00	ND		0,00	0,00	ND		ND		53,41	0,76	ND

profile 2 ICP-OES measurement with Spectro Ametec Arcos II device (SideOnPlasma, 1400W) after sample processing in ultraCALVE IV MLS GmbH with HNO3 at 240°C, 100 bar

depth [cm]	Cr [mg/kg]	Cu [mg/kg]	Fe [mg/kg]	K [mg/kg]	Mn [mg/kg]	Pb [mg/kg]	Zn [mg/kg]
12	31	11	27031	3956	81	82	24
14	47	30	8302	2334	26	302	44
15	44	7	4561	2182	13	280	14
16	16	6	4601	1694	12	252	13
17	3	3	3564	1553	9	251	12
18	20	14	3438	1850	11	281	15
20	2	1	5230	1301	7	217	11
23	17	14	3350	1119	5	187	12
29	17	14	2549	1238	6	106	18
32	21	16	2454	1763	8	78	23
35	20	18	2454	1410	7	58	29
44	55	5	7744	6565	27	31	57
50	65	30	9952	7173	33	26	68
56	65	48	6986	6398	27	17	77

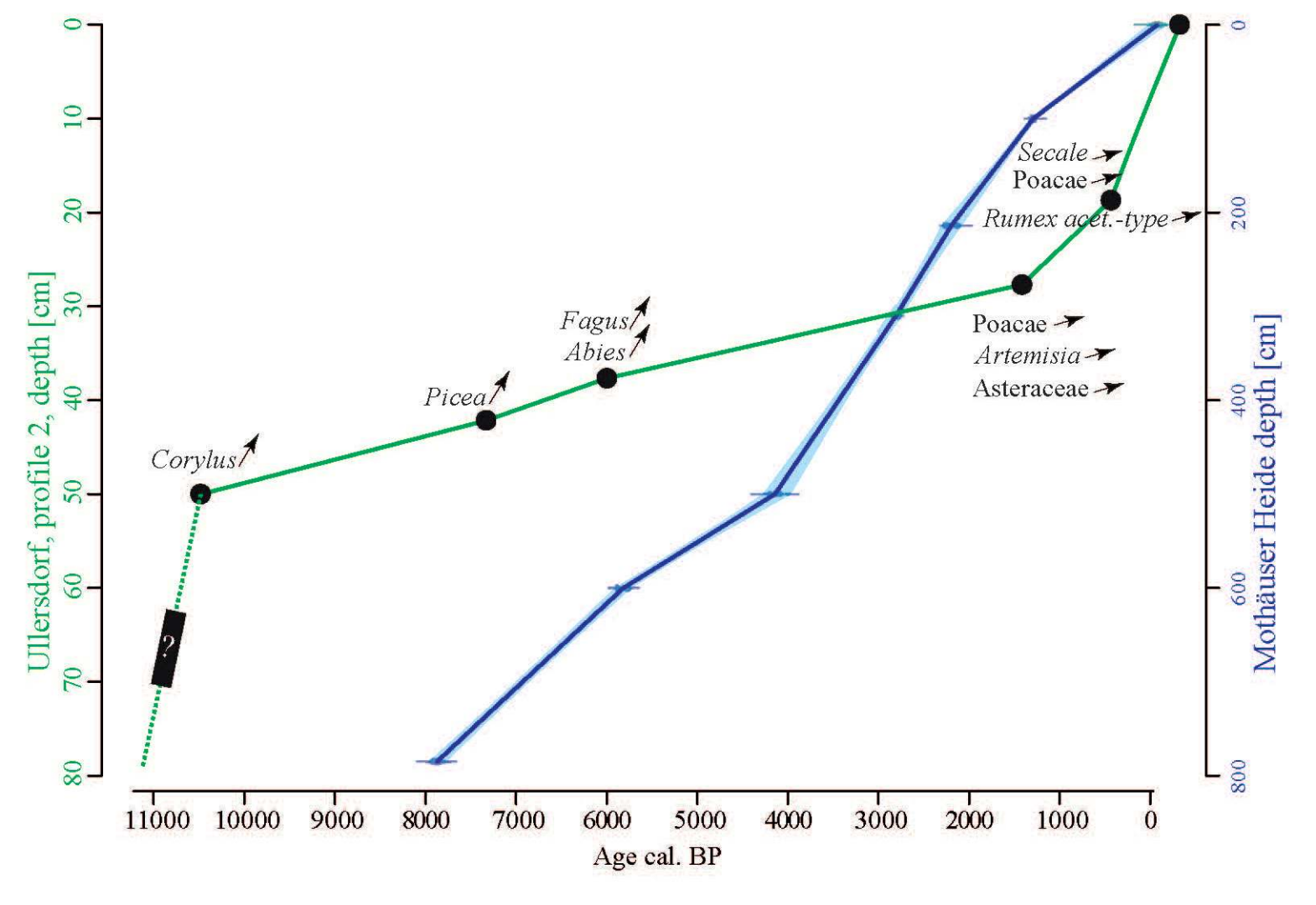
Ullersdorf, profile 2, depth [cm]
0
10
20
30
40
50
60
70
80
Mothäuser Heide depth [cm]
0
200
400
600
800
Corylus
Picea
Fagus
Abies
Secale
Poacae
Rumex acet.-type
Poacae
Artemisia
Asteraceae
?
11000
10000
9000
8000
7000
6000
5000
4000
3000
2000
1000
0
Age cal. BP

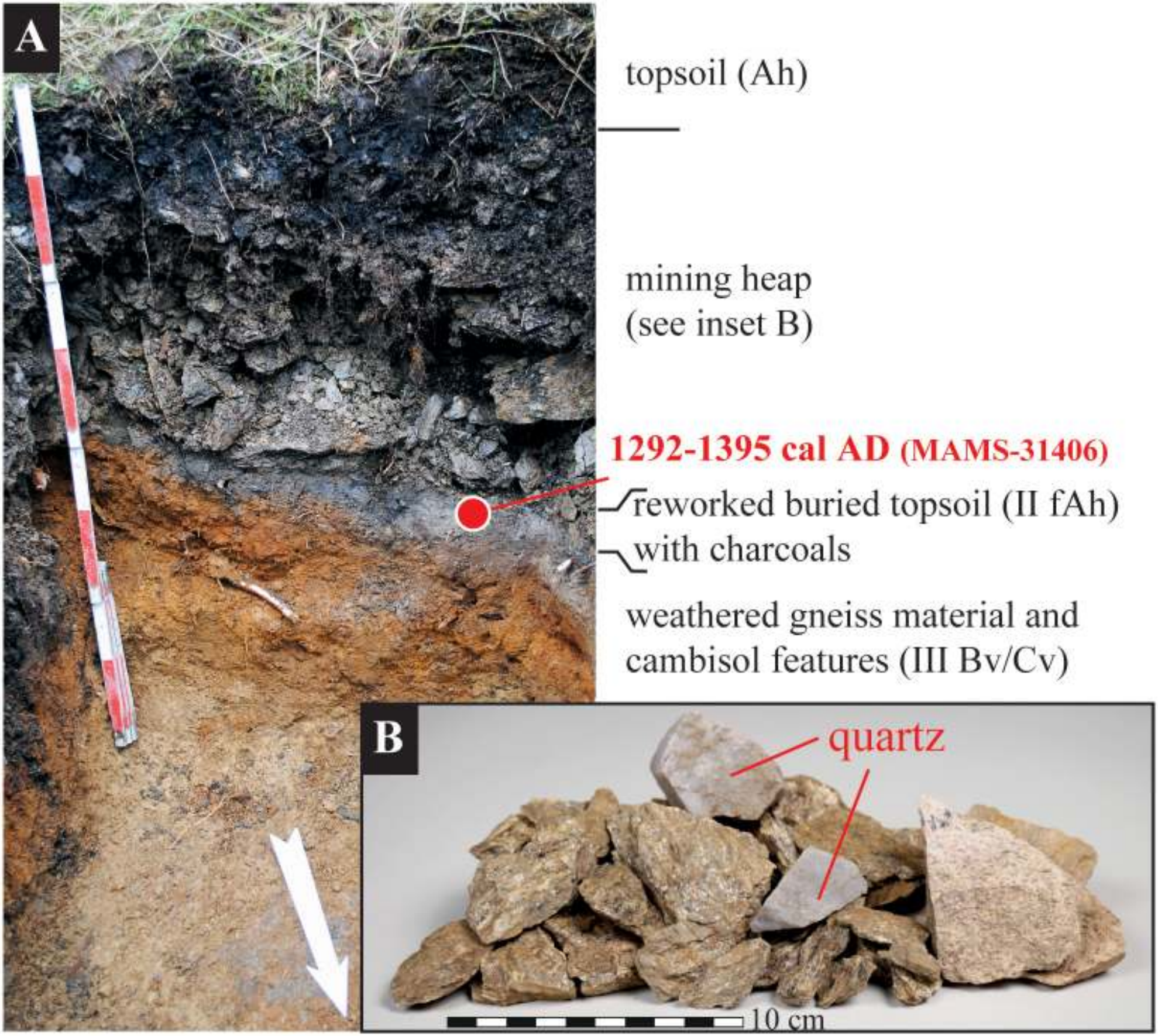
A
topsoil (Ah)
mining heap
(see inset B)
1292-1395 cal AD (MAMS-31406)
reworked buried topsoil (II fAh)
with charcoals
weathered gneiss material and
cambisol features (III Bv/Cv)
B
quartz
10 cm